2022

Re-assessing the Influence of Particle-hosted Sulphide Precipitation on the Marine Cadmium Cycle

Gregory F. de Souza
Institute of Geochemistry and Petrology

Derek Vance
Institute of Geochemistry and Petrology

Matthias Sieber
University of South Florida, sieberm@usf.edu

Tim M. Conway
University of South Florida, tmconway@usf.edu

Susan H. Little
University College London

Available online at www.sciencedirect.com

ScienceDirect

Geochimica et Cosmochimica Acta 322 (2022) 274–296

Geochimica et Cosmochimica Acta

www.elsevier.com/locate/gca

Re-assessing the influence of particle-hosted sulphide precipitation on the marine cadmium cycle

Gregory F. de Souza [a,*], Derek Vance [a], Matthias Sieber [b], Tim M. Conway [b], Susan H. Little [c]

[a] *ETH Zurich, Institute of Geochemistry and Petrology, Clausiusstrasse 25, 8092 Zurich, Switzerland*
[b] *College of Marine Science, University of South Florida, St. Petersburg, FL, USA*
[c] *Department of Earth Sciences, University College London, London, UK*

Received 10 July 2021; accepted in revised form 8 February 2022; Available online 14 February 2022

Abstract

It has been inferred that the marine distributions of the micronutrient cadmium (Cd) and its stable isotope composition (expressed as δ^{114}Cd) bear widespread and unambiguous evidence for loss of Cd from the shallow water column through the formation of particle-associated cadmium sulphide (CdS) in oxygen minimum zones (OMZs). In this review, we bring together elemental and isotopic datasets from the dissolved and particulate Cd pools in order to unravel the multiple, overlapping controls on the distribution of Cd and δ^{114}Cd, and demonstrate that the global dataset challenges this view. By far the most important control on the marine Cd distribution is the extreme plasticity in the cadmium:phosphorus (Cd:P) stoichiometry of biological uptake and, in consequence, particulate export. We show that δ^{114}Cd systematics in low-latitude OMZs that have been taken to reflect Cd loss in fact come about mainly through the interaction between the physical circulation and the variable stoichiometry of biological Cd uptake at high and low latitudes; water-column evidence for Cd loss is thus much less widespread than has previously been inferred. Subtle but consistent signals in particulate elemental and dissolved isotopic data from the open tropical Atlantic and Pacific Oceans allow us to identify the signal of a Cd loss associated with the oxycline of the shallow tropical subsurface, as has previously been suggested. However, this Cd loss appears to be ubiquitous throughout the tropics, rather than confined to oxygen-poor waters, speaking against CdS formation as the driving mechanism. Although its true identity remains unknown, this tropical Cd loss may be related to biological activity. Finally, we show how the processes we consider – the remineralisation of biogenic particles with variable Cd:P stoichiometry, and ubiquitous tropical oxycline Cd loss – bear upon the role of particle-hosted CdS formation in the marine mass balance of Cd, which is likely to be much smaller than recent estimates have suggested.

Keywords: GEOTRACES; Marine biogeochemistry; Southern Ocean; Cadmium sulfide; Oxygen-deficient zone; Cadmium isotopes

Contents

* Corresponding author.
E-mail address: desouza@erdw.ethz.ch (G.F. de Souza).

https://doi.org/10.1016/j.gca.2022.02.009
0016-7037/

1. INTRODUCTION

Despite its known toxicity, culturing studies bear abundant evidence that the metal cadmium (Cd) is beneficial to some marine photosynthesisers, partially relieving growth limitation by zinc in both diatoms and coccolithophorids (Price and Morel, 1990; Lee and Morel, 1995; Lane and Morel, 2000; Xu et al., 2007; Morel, 2013). Certainly, regardless of its exact physiological role, dissolved Cd is taken up by phytoplankton in the sunlit surface ocean, reducing surface concentrations and resulting in a large-scale marine distribution that mimics those of the major nutrients. It has long been known that seawater Cd concentrations are closely correlated with phosphate (PO_4) at the global scale (Fig. 1a; Boyle et al., 1976; Bruland, 1980; Boyle, 1988; de Baar et al., 1994), broadly similar to the canonical Redfield correlation between nitrate (NO_3) and PO_4 (Redfield, 1934).

However, in contrast to the factor ~ 2 variation inferred for the nitrogen:phosphorus ratio of particulate export (12–26 mol/mol; Wang et al., 2019), the cadmium:phosphorus (Cd:P) export ratio has recently been shown to vary by a factor of ~ 7 (0.2–1.5 mmol/mol; Black et al., 2019), while euphotic-zone particulate Cd:P varies by more than 20× (<0.1–2 mmol/mol; Sherrell, 1989; Bourne et al., 2018). This range is likely the result of the extreme plasticity in the stoichiometry of phytoplankton uptake – and, consequently, cellular quota – that is characteristic of Cd and other micronutrients (e.g. Sunda and Huntsman, 2000; Moore et al., 2013; Twining and Baines, 2013). Culture studies with diatoms and coccolithophorids have shown that Cd uptake rates can increase by two orders of magnitude when ambient Cd^{2+} concentrations increase to a similar degree (Lee et al., 1995; Sunda and Huntsman, 1998, 2000). A similar increase is observed in response to low concentrations of free zinc (Zn^{2+}), likely reflecting upregulation of Cd transport to combat Zn limitation (Sunda and Huntsman, 2000; Xu et al., 2007). Growth limitation by iron (Fe) has also been shown to increase the Cd:P of natural phytoplankton assemblages by a factor of 2–10 (Cullen et al., 2003).

This variable uptake stoichiometry plays an important role in creating a much-discussed feature of the marine Cd–PO_4 relationship: the change in its slope in the Atlantic Ocean (Boyle, 1988; de Baar et al., 1994). The increased data coverage of the GEOTRACES era has allowed confirmation and combination of two early hypotheses that (a) variation in the Cd:P of biological uptake (Saager and de Baar, 1993; de Baar et al., 1994), and (b) the low Cd:PO_4 of upper-ocean waters exported from the Southern Ocean (Frew and Hunter, 1992; Frew, 1995) are dominantly responsible for this slight non-linearity (Baars et al., 2014; Quay et al., 2015). Detailed Southern Ocean studies have shown that elevated phytoplankton uptake of Cd relative to PO_4 south of the Antarctic Polar Front (APF) produces a signal of relative Cd depletion in surface waters of the Subantarctic Zone, a signal that is transmitted to mode and intermediate waters that form in this region (Ellwood, 2008; Abouchami et al., 2014; Baars et al., 2014; Sieber et al., 2019a). Basin-scale meridional transects have shown that these upper-ocean waters transport the Southern Ocean signal of relative Cd depletion into the low-latitude upper ocean, eventually transmitting it to North Atlantic Deep Water (Xie et al., 2015; Middag et al., 2018; Sieber et al., 2019b). As such, the first-order controls on the marine Cd distribution (Roshan and

DeVries, 2021) are similar to those governing the distributions of other macro- and micronutrients and their isotopes (Sarmiento et al., 2004; 2007; Weber and Deutsch, 2010; de Souza et al., 2012; Martiny et al., 2013; Vance et al., 2017; Fripiat et al., 2021).

While resolving such long-standing questions, GEOTRACES-era data have also revealed new details of the marine Cd–PO_4 relationship, now often studied using the tracer Cd*, which quantifies the deviation of Cd concentration from a linear correlation with PO_4 (Eq. (1) in Section 3.1). These data have shown that oxygen minimum zones (OMZs) are major exceptions to the open-ocean Cd–PO_4 correlation: in a Cd–PO_4 cross-plot, data from the uppermost OMZ fall below the trend defined by

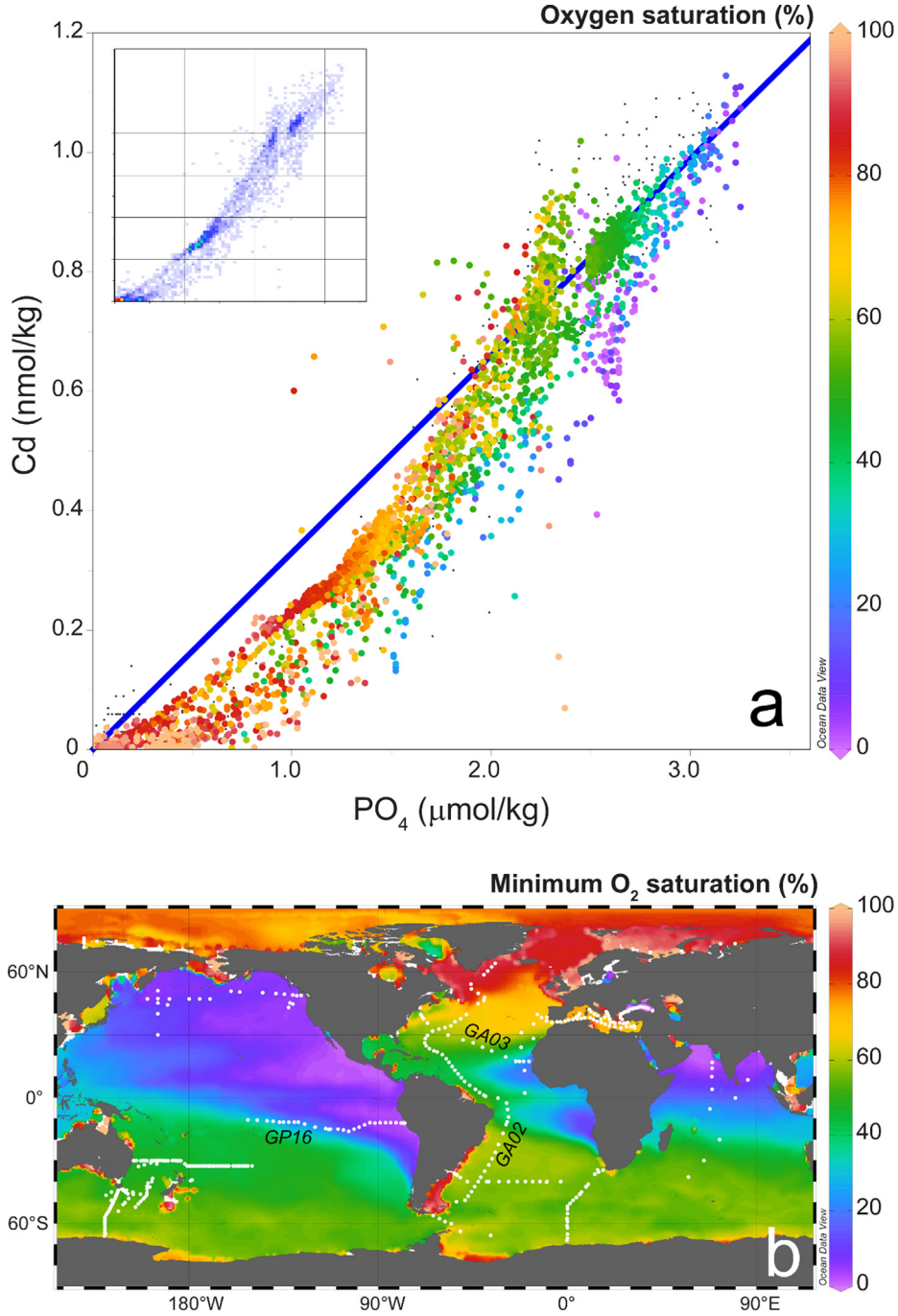

Fig. 1. (a) Cross-plot of Cd against PO_4 for all data available in the GEOTRACES Intermediate Data Product 2017 (ver. 2; Schlitzer et al., 2018), coloured by oxygen saturation. Black points indicate data for which no O_2 data is available; blue line is 0.33*PO_4 and marks Cd* = 0 nmol/kg (Eq. (1)); inset shows data density. (B) Locations of stations with Cd data (white circles) overlain on a map of minimum water-column O_2 saturation (Garcia et al., 2013); GEOTRACES sections often referred to in the text are labelled. Figure created using Ocean Data View 5 (Schlitzer, 2019).

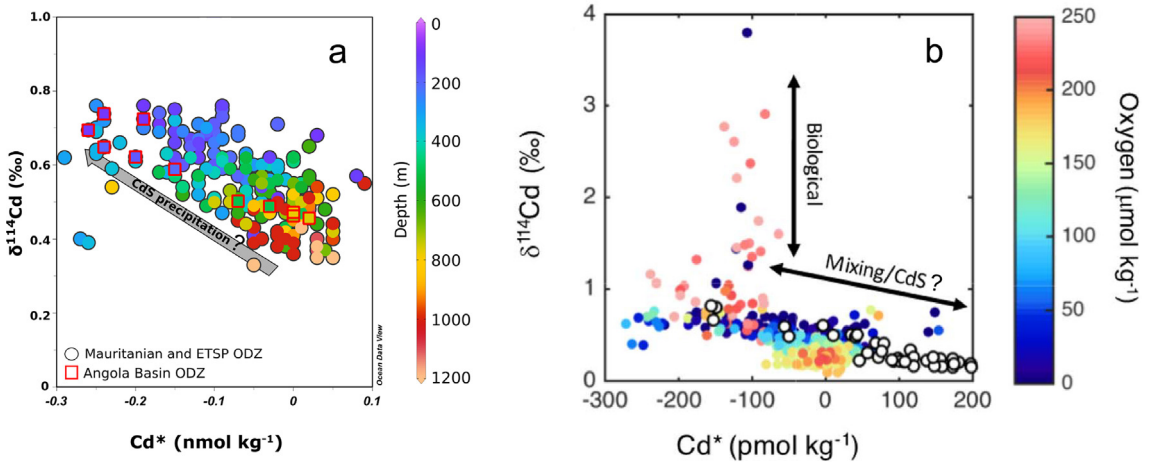

Fig. 2. Figures modified from (A) Guinoiseau et al. (2019) showing tropical OMZ Cd*-δ^{114}Cd correlations and (B) John et al. (2018) showing the similarity between the Peruvian OMZ Cd*-δ^{114}Cd correlation (colours) and that in the Southern Ocean (white; data from Abouchami et al., 2011; Xue et al., 2013).

well-oxygenated waters (Fig. 1a), indicating an apparent deficit in Cd relative to PO_4. It has been proposed that this offset reflects a loss of dissolved Cd at the upper OMZ boundary, through the precipitation of cadmium sulphide (CdS) in sulphidic microenvironments within sinking and decomposing biogenic particles (Janssen et al., 2014; Conway and John, 2015a). Such apparent Cd deficits, identified by a decrease in Cd* values, have been observed in the OMZs of the eastern tropical North and South Atlantic (Waeles et al., 2013; Conway and John, 2015a; Wu and Roshan, 2015; Guinoiseau et al., 2019; Xie et al., 2019a), in the oxygen-poor shallow subsurface of the subarctic Pacific (Janssen et al., 2014; Janssen et al., 2017; Yang et al., 2018), and in the OMZ of the eastern tropical South Pacific (John et al., 2018). The interpretation of these signals as resulting from CdS formation is consistent with evidence for dynamic sulphur cycling within O_2-depleted oceanic OMZs (e.g. Canfield et al., 2010; Ulloa et al., 2012) and with particulate data showing a complementary enrichment in Cd relative to P in the North Atlantic OMZ (Janssen et al., 2014; Conway and John, 2015a; Waeles et al., 2016; Bianchi et al., 2018).

However, the factor 10–20 variability in the Cd:P stoichiometry of marine particulates (Twining et al., 2015; Bourne et al., 2018; Lee et al., 2018) and particulate export fluxes (based on particles > 51 µm; Black et al., 2019) introduces a key ambiguity to the interpretation of Cd* in OMZs, which host large inventories of regenerated nutrients that have accumulated through decomposition of organic matter. Within OMZs, lower concentrations of Cd than would be expected from the deep-ocean Cd–PO_4 relationship – i.e., negative Cd* values – may simply result from remineralisation of organic matter with a low Cd:P ratio, and may be further complicated by non-stoichiometric release of Cd and P from decomposing particles (Bourne et al., 2018; Xie et al., 2019a; Cloete et al., 2021; Roshan and DeVries, 2021). Indeed, Wu and Roshan (2015) and Roshan and Wu (2015) have ascribed the apparent Cd deficit in the North Atlantic OMZ to precisely such remineralisation of relatively Cd-poor material, rather than to absolute Cd loss.

A key piece of evidence supporting the inference of particle-hosted CdS precipitation in OMZs has come from the stable isotope composition of dissolved Cd (expressed as δ^{114}Cd relative to the standard NIST-3018). In low-latitude OMZs of the Atlantic and the Pacific, dissolved δ^{114}Cd exhibits an increase that correlates with decreasing Cd* (Fig. 2a; Janssen et al., 2014; Conway and John, 2015a; John et al., 2018; Guinoiseau et al., 2019; Xie et al., 2019a). Such a δ^{114}Cd elevation would be expected to result from CdS formation, given the preferential incorporation of lighter Cd isotopes into CdS observed in laboratory experiments (Guinoiseau et al., 2018). Indeed, Guinoiseau et al. (2018; 2019) have shown that the δ^{114}Cd–Cd* correlations in the low-latitude Atlantic and Pacific OMZs are consistent with fractionation into CdS (Fig. 2a), and infer that CdS precipitation plays an important role in Cd cycling in all OMZs. Scaling the results of the optimised particle model of Bianchi et al. (2018), Guinoiseau et al. (2019) suggest that the associated marine sink is at least as large as other known sinks of Cd (sub- or anoxic sediments, e.g. Morford and Emerson, 1999; Little et al., 2015), and that it could be the dominant sink in the marine mass balance of Cd.

However, phytoplankton uptake of Cd also favours its lighter isotopes, such that under Cd-replete conditions, euphotic-zone uptake produces an elevated δ^{114}Cd value in residual surface-ocean dissolved Cd (Lacan et al., 2006; Ripperger et al., 2007; Abouchami et al., 2011; Xue et al., 2013). Thus, the same strong Southern Ocean drawdown that slightly decouples the Cd and PO_4 distributions, producing a low-Cd* signal in upper-ocean water masses formed in the Southern Ocean (Baars et al., 2014), also introduces a preformed signal of elevated δ^{114}Cd into these water masses (Sieber et al., 2019a). Their northward transport influences the low-latitude δ^{114}Cd and Cd* distributions (Abouchami et al., 2014; Baars et al., 2014; Conway and John, 2015a; Xie et al., 2015; 2017; Middag et al.,

2018; George et al., 2019; Sieber et al., 2019b), and John et al. (2018) have pointed out that the δ^{114}Cd–Cd* correlation of the Peruvian OMZ is near-identical to the preformed covariation observed in Southern Ocean waters (Fig. 2b). Conversely, no δ^{114}Cd–Cd* correlation is observed in the subarctic Pacific (Janssen et al., 2017; Yang et al., 2018), although it also hosts extremely low shallow-subsurface O_2 (<20 μmol/kg). Janssen et al. (2017) argue that this absence may be a consequence of the high Cd concentrations here, but it is worth noting that this region is not influenced by upper-ocean waters of Southern Ocean origin (Sarmiento et al., 2004).

Together, these observations highlight fundamental ambiguities in water-column evidence that has been interpreted as reflecting particle-hosted CdS precipitation within OMZs: first, the close correlation between Cd* and δ^{114}Cd (Fig. 2) may simply be a distally-produced signal of fractionating biological uptake at high Cd:P, rather than reflecting local processes; and second, the trend towards low or negative Cd* values within OMZs could result from the accumulation of a regenerated signal with low Cd:PO_4 within their large remineralised nutrient pools.

This review brings together a range of published datasets in order to deconvolve the competing controls on Cd in low-latitude OMZs. We do so using a data analysis approach that takes into account the large-scale structure of the dissolved Cd* and δ^{114}Cd distributions, as well as the integrated signal of regeneration. A novel element of our synthesis is the consideration of the water-column data in the context of published particulate datasets and their systematics. Our re-assessment reveals little water-column evidence for particle-hosted CdS formation, which likely plays only a small role in the marine mass balance of Cd.

2. DATASETS AND SOURCES

This study is based on published open-ocean GEOTRACES-era datasets, available via the GEOTRACES Intermediate Data Product 2017 (IDP2017v2; Schlitzer et al., 2018) or individual publications, with particular focus on dissolved Cd datasets that include δ^{114}Cd observations. Dissolved-phase Southern Ocean data are from the circumpolar datasets of Sieber et al. (2019a) and Janssen et al. (2020). In the South Pacific, we focus on two GEOTRACES transects: GP19, which extends northwards from the Southern Ocean into the western tropical Pacific (Sieber et al., 2019b), and the zonal transect GP16 from the western tropical Pacific to the South American coast (John et al., 2018). Atlantic data are from the GA02 transect that extends northwards from the Southern Ocean along the western Atlantic (Xie et al., 2015; 2017; Middag et al., 2018), as well as from tropical waters of the equatorial region (GA11; Xie et al., 2019a), the South Atlantic OMZ (GA08; Guinoiseau et al., 2019), and the North Atlantic OMZ (GA03; Conway and John, 2015a). We do not consider the tropical Atlantic [Cd] data of Waeles et al. (2013; 2016), since they report total dissolvable Cd from unfiltered samples. The Indian Ocean Cd concentration, [Cd], data of Vu and Sohrin (2013) are only briefly discussed, since they are not accompanied by δ^{114}Cd or particulate Cd data. Particulate data we consider are from transects GP16 and GA03 (Twining et al., 2015; Ohnemus et al., 2017; Lee et al., 2018; Black et al., 2019) and the compilation of Bourne et al. (2018). GEOTRACES intercalibration indicates that the inter-laboratory reproducibility of seawater δ^{114}Cd is ± 0.07‰ ($2\sigma_{SD}$). Reported $2\sigma_{SD}$ uncertainties on PO_4 concentration, [PO_4], measurements are ± 0.02 μmol/kg (e.g. Rijkenberg, 2011); for [Cd] determined by isotope dilution, published data indicate $2\sigma_{SD}$ uncertainties of ± 0.01 nmol/kg at concentrations ~ 0.25 nmol/kg and ± 0.03 nmol/kg at deep-water Cd concentrations of ~ 1 nmol/kg (Boyle et al., 2012; Middag et al., 2015); together, these suggest a maximum propagated $2\sigma_{SD}$ of ± 0.03 nmol/kg for Cd*.

3. DISCUSSION

Correlations between δ^{114}Cd and Cd* in low-latitude OMZs have been interpreted to unambiguously reflect CdS formation. In the following, we consider the strengths and ambiguities of Cd* (Section 3.1) and review the Southern Ocean control on the Cd distribution in order to assess its influence on low-latitude δ^{114}Cd–Cd* correlations (Section 3.2). Combining dissolved and particulate Cd data, we examine the low-latitude alteration of the [Cd], Cd* and δ^{114}Cd distributions in the tropical South Pacific (Section 3.3) and tropical Atlantic (Section 3.4). We synthesise our findings in Section 3.5, and discuss their implications for the role of particle-hosted CdS formation in the marine Cd budget in Section 3.6.

3.1. Tracing Cd cycling with Cd*

*3.1.1. Definition of Cd**

First applied by Baars et al. (2014), Cd* is an extension to cadmium of a concept previously applied to the major nutrients (Gruber and Sarmiento, 1997; Sarmiento et al., 2004; 2007). The aim of such "star"-tracers, produced by linear combination of two biogeochemically-cycled elements, is to eliminate a major source of large-scale variability, thus bringing into focus variations specific to the element of interest (Gruber and Sarmiento, 1997). For Cd*, this linear combination is:

$$Cd^* = [Cd]_{obs} - (Cd/PO_4)_{ref} \times [PO_4]_{obs} \quad (1)$$

Thus, Cd* reflects the deviation of the observed Cd concentration, $[Cd]_{obs}$, from that expected from the observed PO_4 concentration ($[PO_4]_{obs}$) multiplied by a reference ratio, $(Cd/PO_4)_{ref}$. Authors have chosen different values for $(Cd/PO_4)_{ref}$, typically choosing the local deep water value, such that in published definitions of Cd* its value ranges from 0.25 mmol/mol (Atlantic Ocean, e.g. Conway and John, 2015a) to 0.54 mmol/mol (Southern Ocean; Baars et al., 2014). However, a normalisation to local deep water Cd:PO_4 implies a direct connection between local deep- and upper-ocean waters, which is not true over most of the ocean (e.g. Sarmiento et al., 2004).

In our opinion, a single, globally relevant value of $(Cd/PO_4)_{ref}$ should be applied regardless of study area: we suggest 0.33 mmol/mol, a value that characterises the

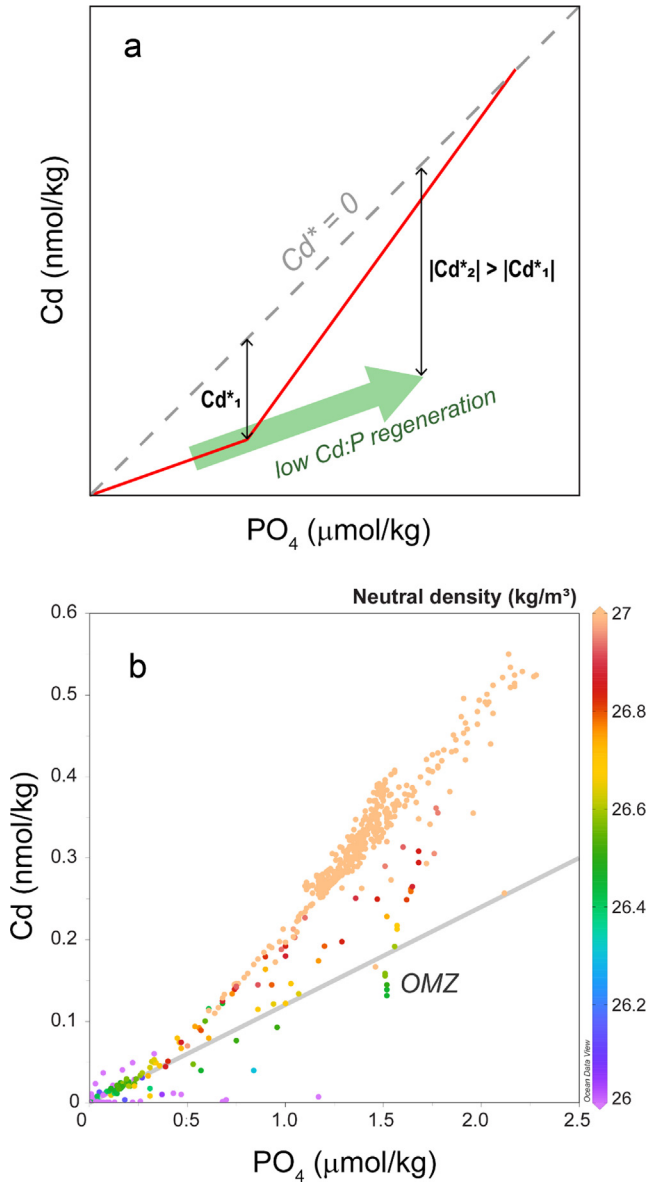

Fig. 3. (A) Schematic illustrating the influence of regeneration of low Cd:P material on Cd*. Oxygen-depleted waters may bear more negative Cd* values (Cd^*_2) simply because they contain higher concentrations of regenerated Cd and PO_4, from regenerated biomass with low Cd:P, than better-ventilated waters (Cd^*_1). (B) Example for North Atlantic OMZ (Conway and John, 2015a) showing that the low Cd* datapoints of the OMZ lie very close to the grey Cd:PO4 line (0.12 mmol/mol) defining better-ventilated waters of the same density (see colour shading).

Cd-rich deep ocean (mean of IDP2017v2 data > 2000 m, excluding the Atlantic Ocean: 0.33 ± 0.02, n = 474; Schlitzer et al., 2018) and thus assigns a Cd* of 0 nmol/kg to most of the deep ocean, with the (meaningful) exception of much of the Cd-poor deep Atlantic (Fig. 1a). Such a definition of Cd* encodes an *expected mean behaviour* of Cd, i.e. that its concentration scales with that of PO_4 according to the ratio of their mean deep-ocean concentrations, allowing Cd* to be interpreted as a measure of the decoupling of the distribution of Cd from that of PO_4. A globally uniform definition of Cd* also permits comparison between basins, revealing highly systematic similarities (Sections 3.2 and 3.4).

3.1.2. Cd* in OMZs: special considerations

It is important to note that the absolute value of Cd* is arbitrary and cannot be directly associated with Cd loss or addition. Preformed variations in Cd* inherited from the surface ocean due to behaviour that deviates from the *expected mean* (e.g. uptake at $Cd:PO_4 > 0.33$ mmol/mol) will lead to ocean-interior Cd* variation that is unrelated to local loss/addition processes. Thus, vertical Cd* variations at any one location cannot be attributed to addition or loss without consideration of the preformed structure of the Cd* distribution, especially in the upper ocean.

Wu and Roshan (2015) brought to light a second important characteristic of Cd*. These authors noted that,

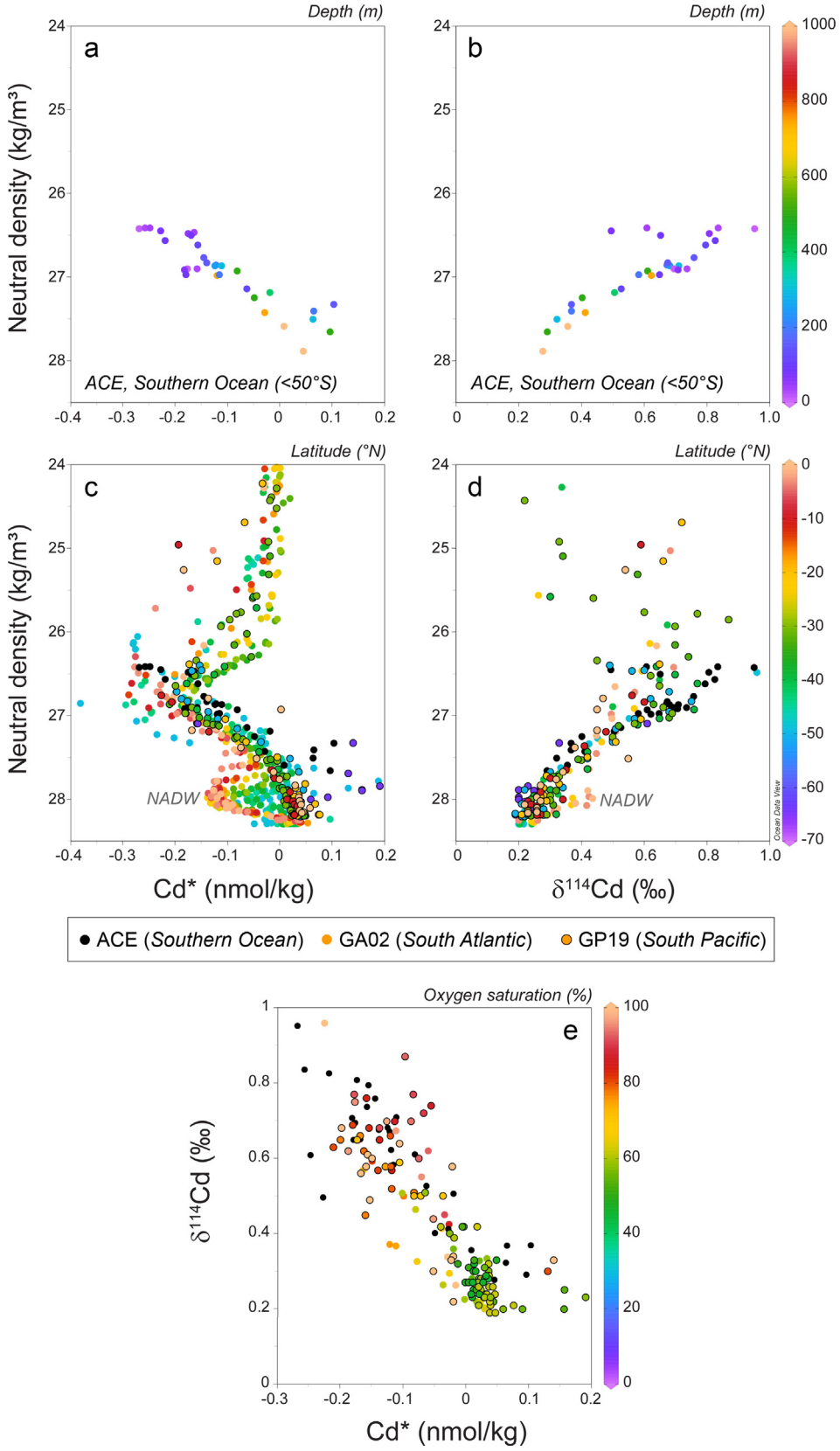

Fig. 4. Subantarctic isopycnal distributions of (A) Cd* and (B) δ^{114}Cd from north of 50°S in the Southern Ocean (Sieber et al., 2019a; Janssen et al., 2020); isopycnal distributions of (C) Cd* and (D) δ^{114}Cd systematics along the meridional transects GA02 (Xie et al., 2017; Middag et al., 2018) and GP19 (Sieber et al., 2019b) in the South Atlantic and South Pacific respectively. (E) Cd*-δ^{114}Cd systematics for the Southern Ocean (<50°S; Sieber et al., 2019a) and well-ventilated subtropical waters of the South Pacific (>19°S; Sieber et al., 2019b) and South Atlantic (>20°S; Xie et al., 2017).

although data from the North Atlantic OMZ fall off the steep Cd–PO_4 trend observed at high [PO_4] (Fig. 3b), these waters in fact bear the same dissolved Cd:PO_4 ratio as other shallow waters. Their anomalous behaviour in a Cd–PO_4 cross-plot results simply from the fact that, being OMZ waters with large pools of regenerated nutrients, they plot at relatively high *concentrations* of both Cd and PO_4. Thus, Wu and Roshan (2015) argue that the OMZ waters simply extend the shallow-water Cd–PO_4 trend to higher concentrations, due to the regeneration of particles with low Cd:P. Since Cd* is the linear combination of two concentrations, it will become more negative as [Cd] and [PO_4] increase along a trend with slope lower than $(Cd/PO_4)_{ref}$ (Fig. 3a), documenting remineralisation at a Cd:P below the *expected mean* of 0.33 mmol/mol. Given the large variability in particulate Cd:P stoichiometry (Twining and Baines, 2013; Bourne et al., 2018), the potential for such a driver of Cd* trends needs to be recognised, especially in OMZs. Furthermore, the concentration-dependence of Cd* predisposes it to display strong vertical variations in tropical OMZs, where nutrient-rich OMZ waters are typically overlain by nutrient-depleted tropical waters bearing near-zero Cd*.

3.2. High-latitude influence on the low-latitude δ^{114}Cd–Cd* correlation

Due to the fact that the conversion pathway of upwelling deep waters to upper-ocean waters passes through the *surface* Southern Ocean, the stoichiometry of biological uptake in this region has an outsize influence on the marine distributions of biologically-relevant elements (Sarmiento et al., 2004; 2007). Recent research has clearly shown that Cd is no exception to this general rule (Ellwood, 2008; Abouchami et al., 2014; Baars et al., 2014; Quay et al., 2015; Xie et al., 2015; Middag et al., 2018; George et al., 2019; Sieber et al., 2019b). South of the APF, the shallow-water Cd:PO_4 relationship suggests a highly elevated Cd:PO_4 uptake/regeneration ratio of $\sim$ 1.05 mmol/mol (Sieber et al., 2019a), consistent with surface-ocean particulate Cd:P north and south of the APF in summer (0.86–2.32 mmol/mol in non-Fe-amended waters during SOFeX; Bourne et al., 2018) as well as winter (0.86–1.07 mmol/mol at 25 m; Cloete et al., 2021). This elevated uptake leads to a decoupling of [Cd] and [PO_4] in Subantarctic surface waters (Ellwood, 2008; Baars et al., 2014): here, [Cd] drops to close to zero while [PO_4] is $\sim$ 0.5 μmol/kg, resulting in a Cd* value of around −0.2 nmol/kg. A recent circumpolar dataset (Sieber et al., 2019a; Janssen et al., 2020) has shown that this Subantarctic Cd* signal is visible in all sampled sectors of the Southern Ocean (Fig. 4a). Due to biological isotope fractionation, the negative Cd* signal is coupled to elevated δ^{114}Cd (Abouchami et al., 2011; Xue et al., 2013; George et al., 2019; Sieber et al., 2019a), with values up to + 1‰ in the summer mixed layer (Fig. 4b).

Two GEOTRACES sections extending northward from the Southern Ocean, through the well-ventilated western sides of the South Atlantic (GA02: Xie et al., 2017; Middag et al., 2018) and South Pacific (GP19: Sieber et al., 2019b), have demonstrated the larger-scale influence of Southern Ocean uptake on the [Cd], Cd*, and δ^{114}Cd distributions. Fig. 4 plots these data against neutral density (γ^n), allowing an isopycnal view that highlights the extremely close similarity between the Cd* distributions in the subtropical South Atlantic and South Pacific (Fig. 4c). Both distributions exhibit a Cd* minimum of about −0.2 nmol/kg centred around γ^n = 26.8–27 kg/m^3, the density of Southern Ocean mode waters that are formed in the Subantarctic Zone (McCartney, 1982) and carry this signal of Southern Ocean uptake well into subtropical latitudes (Figs. S1 and S2; e.g. Baars et al., 2014; Xie et al., 2015). The elevated δ^{114}Cd in the subtropical Pacific and Atlantic thermocline (Fig. 4d) results from the high δ^{114}Cd of these upper-ocean waters bearing negative Cd* (Abouchami et al., 2014; Xie et al., 2017; George et al., 2019; Sieber et al., 2019b).

While recognising the similarity between the δ^{114}Cd–Cd* correlations in the Peruvian OMZ and the Southern Ocean (Fig. 2b), John et al. (2018) remained agnostic as to whether the correlation off Peru reflected low- or high-latitude processes. The Cd systematics in the O_2-rich western South Pacific and South Atlantic clearly identify the source of this correlation as the Southern Ocean. The strong influence of Southern Ocean uptake on the preformed distributions of Cd* and δ^{114}Cd is particularly clear in a cross-plot of Cd* and δ^{114}Cd within the western subtropical South Pacific and South Atlantic (Fig. 4e). These well-ventilated waters exhibit a correlation very similar to that observed in the poorly-ventilated eastern OMZs (Fig. 2a) – and essentially identical to that observed within the Southern Ocean itself (Fig. 4e).

Thus, a δ^{114}Cd–Cd* correlation is not unambiguous proof of subsurface Cd loss. On the contrary, such a correlation seems to be a typical feature of ocean regions influenced by upper-ocean waters of Southern Ocean origin. The presence of such structure in the Cd* and δ^{114}Cd distributions precludes analysis of their systematics in a framework that ignores the spatial dimension, such as the δ^{114}Cd–Cd* cross-plots of Fig. 2. Rather, identifying the influence of low-latitude processes requires an approach that takes into account their preformed distributions. This may be done using models (e.g. Roshan et al., 2017), but due to the fine vertical scale of the signals of interest, we take a data-based approach in this contribution.

3.3. South Pacific low-latitude cycling

Focusing in on the South Pacific, we now consider how the Cd distribution changes from the well-ventilated subtropics along GEOTRACES transect GP19 (Fig. 4; Sieber et al., 2019a) into the increasingly poorly ventilated tropical waters along transect GP16 (John et al., 2018). This latter transect begins in the tropical South Pacific east of GP19 (Fig. 5h), and extends eastward into the OMZ off the Peruvian coast, where minimum O_2 concentrations reach the low nanomolar range (e.g. Tiano et al., 2014). At $\sim$ 100°W, GP16 encounters a density-compensated front that separates the OMZ from better-ventilated waters to the west. The waters to the west are still firmly within the trop-

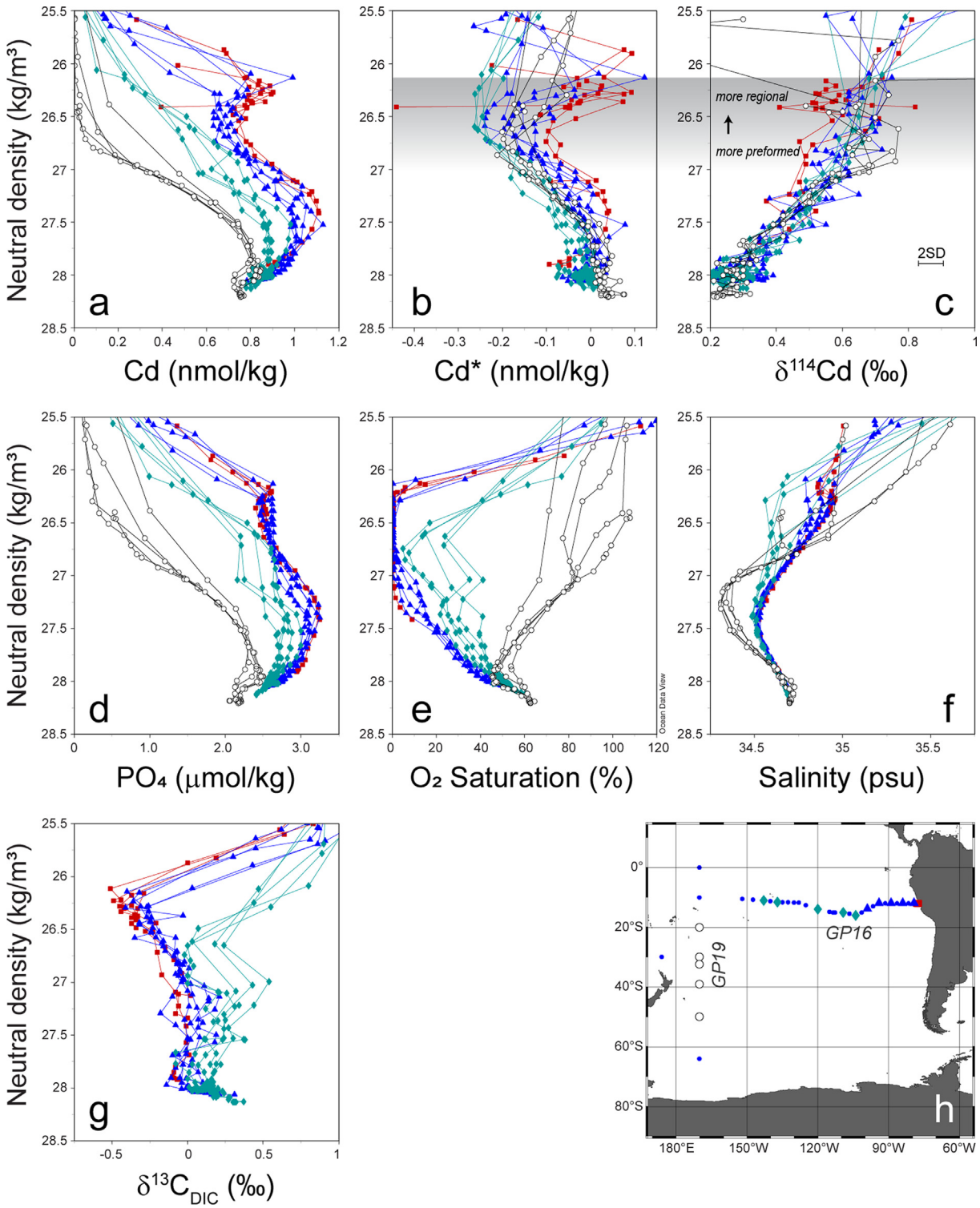

Fig. 5. Subtropical-tropical isopycnal systematics of the South Pacific from GEOTRACES sections GP19 (Sieber et al., 2019b) and GP16 (John et al. 2018; Schlitzer et al., 2018). White circles: subtropical western Pacific; teal diamonds: open tropical Pacific (west of 100°W); blue triangles: OMZ waters (east of 100°W), red squares : shelf/slope waters (OMZ waters over shelf or slope; GP16 Stas 2–5). Grey shaded area in panels **b** and **c** schematically shows the increasing upward alteration of preformed Cd* and δ^{114}Cd signals by regional ones (see main text). Smaller blue circles represent stations with δ^{114}Cd data that are not shown here.

ical Pacific, as highlighted by the marked oxygen minimum, not present in the subtropical gyre, that extends across the entire transect along $\gamma^n = 26.65–26.75$ kg/m^3 (Figs. 5e and S3). West of 100°W, in what we denote the "open tropical

Pacific", minimum O_2 concentrations are 50–75 μmol/kg, while to the east they are below the detection limit of 2 μmol/kg (Cutter et al., 2018).

3.3.1. Subtropical-tropical comparison

Fig. 5 presents the isopycnal distributions of [Cd], Cd* and δ^{114}Cd in the subtropical waters along GP19 (Sieber et al., 2019b) and the tropical waters along GP16 (John et al., 2018). There is a marked increase in [Cd] from the subtropics to the O_2-poorer tropics over almost the entire water column (Fig. 5a); especially in the upper ocean, this increase becomes more marked towards the east. Waters of the OMZ and over the shelf/slope also show a [Cd] maximum, only weakly seen in PO_4 (Fig. 5d), at $\gamma^n \approx 26.25$ kg/m^3, coinciding with the base of the oxycline (Fig. 5e). In contrast to the large [Cd] increases between the subtropics and tropics, tropical Cd* and δ^{114}Cd show only small variations from the structure in the subtropical data (Fig. 5b,c; Section 3.2). This is not surprising, since Cd* is designed to remain invariant in the face of *expected mean* regeneration (Eq. (1)), and regeneration has little leverage to alter interior δ^{114}Cd, especially in the Cd-rich Pacific (e.g. Janssen et al., 2017; Yang et al., 2018; Sieber et al., 2019b). As a consequence, the Cd* and δ^{114}Cd distributions more strongly reflect the large-scale Southern Ocean control reviewed in Section 3.2.

Nonetheless, in the upper tropical ocean, Cd* shows significant differences to the subtropical distribution, deviating from it at densities less than 26.8 kg/m^3 (~350 m) in the open tropical Pacific, and at densities less than ~ 27.25 kg/m^3 (~625 m) within the OMZ (Fig. 5b). Especially in the open tropical Pacific and towards the outer OMZ, the Cd* minimum along GP16 is seen at slightly shallower depths than in the subtropics, and Cd* values are more negative as well (Fig. 5b). In addition, there is a steady isopycnal increase in upper-ocean Cd* eastward, towards more poorly ventilated waters. Finally, waters east of 100°W also bear shallow Cd* *maxima* corresponding to the abovementioned [Cd] maxima (Fig. 5a,b). In these shallow maxima (40–120 m water depth), Cd* reaches up to + 0.1 nmol/kg, coinciding with the base of the oxycline (Fig. S4). Values of δ^{114}Cd, which are generally very similar to the southern subtropics (George et al., 2019; Sieber et al., 2019b), show little variation except for a slight decrease in shelf/slope waters (Fig. 5c).

3.3.2. Influence of remineralisation in the South Pacific OMZ

For the following, it is important to bear in mind the fact that an isopycnal approach has some limitations in a comparison of the subtropical and tropical Pacific. Tropical dynamics in the zonally expansive Pacific lead to significant cross-isopycnal fluxes in the interior, resulting for instance in the weakening of the AAIW salinity minimum between the subtropics and tropical Pacific (Fig. 5f; Tsuchiya and Talley, 1996; Fiedler and Talley, 2006). Southern-sourced Cd* minima will similarly be weakened by diapycnal mixing in the tropics, while tropical Cd and nutrient distributions are also influenced by the contribution of North Pacific waters to the equatorial Pacific thermocline (Johnson and McPhaden, 1999; Dugdale et al., 2002; Schott et al., 2004).

Nonetheless, since the only sources of deep water (>2000 m) to the Pacific are the Southern Ocean water masses flowing northward in the abyssal western Pacific (e.g. Reid, 1997), the marked increase in [Cd] over most of the tropical Pacific water column (Fig. 5a) highlights the strong influence of regeneration on the tropical Cd distribution (Roshan et al., 2017). This is especially true for the densities hosting the OMZ, where [Cd] increases by ~ 0.8 nmol/kg relative to the southern subtropics (Fig. 5a). Some proportion of this increase is likely due to the abovementioned North Pacific contribution. Limited data from the well-ventilated subtropical North Pacific (Yang et al., 2018) suggest that these waters bear much higher [Cd] near OMZ densities (~0.4 nmol/kg at 26.5 kg/m^3) than corresponding South Pacific waters (~0.05 nmol/kg), and their influence may thus partially explain the higher tropical [Cd].

However, a process that certainly also plays a role, especially in the OMZ and over the shelf/slope, is the regional regeneration of Cd from the large export fluxes of the productive equatorial and coastal upwelling regimes (e.g. Honjo et al., 2008). This is unequivocally shown by the stable isotope composition of dissolved inorganic carbon (DIC), $\delta^{13}C_{DIC}$, which exhibits values ~ 1‰ lower within OMZ and shelf/slope waters than in the open tropical Pacific (Fig. 5g; to our knowledge, no $\delta^{13}C_{DIC}$ data are available for GP19). This shift documents the accumulation of isotopically light, regionally regenerated DIC within the OMZ (e.g. Schmittner et al., 2013), and coincides with lower δ^{114}Cd values in shelf/slope waters (Fig. 5c,g). Tellingly, the regeneration-driven subsurface $\delta^{13}C_{DIC}$ *minimum* coincides near-exactly with the shallow subsurface *maxima* in [Cd] and Cd* east of 100°W (Fig. 5a,b,g), fingerprinting the remineralisation of organic matter with a Cd:P significantly higher than the *expected mean* of 0.33 mmol/mol (Section 3.1). Indeed, particulate data compiled by Bourne et al. (2018) show that the Cd:P of euphotic-zone particles along GP16 increases from 0.03 mmol/mol in the oligotrophic open tropical Pacific to as high as 1.42 mmol/mol within the upwelling region above the OMZ. More generally, seasonal and interannual variability documented by Bourne et al. (2018) shows that Pacific euphotic-zone particles have higher Cd:P when productivity is higher. Remineralisation of particles with the high Cd:P observed in the productive Peruvian upwelling will increase subsurface Cd*, as is indeed observed for all waters that bear the tropical remineralisation signal in $\delta^{13}C_{DIC}$ (Fig. 5b,g). The slightly lower δ^{114}Cd values in shelf/slope waters over this density range suggest that incomplete Cd utilisation in the upwelling region above the innermost OMZ results in the export of isotopically light particulate Cd, analogous to the low particulate δ^{114}Cd observed in the productive subarctic Pacific (Yang et al., 2018; Janssen et al., 2019).

Thus, the main low-latitude influence on the Cd distribution in the southern tropical Pacific is the remineralisation of organic matter. Within the Peruvian OMZ itself,

this organic matter is especially Cd-rich relative to the *expected mean*, resulting in a strong elevation of [Cd] and Cd*, while δ^{114}Cd shows a muted opposite response. Thus, even in the functionally anoxic waters of the Peruvian OMZ, and its associated oxycline, in which a diverse microbial community undertakes a variety of spatially-compressed redox processes including sulphur cycling (Canfield et al., 2010; Ulloa et al., 2012), remineralisation of Cd-rich particles has a much larger influence on the Cd distribution than loss of Cd to sulphides (Janssen et al., 2014), deep-living prokaryotes (Ohnemus et al., 2017) or adsorption to particles (Lee et al., 2018). Since remineralisation has limited leverage to alter δ^{114}Cd, the OMZ δ^{114}Cd distribution is largely driven by the preformed upper-ocean δ^{114}Cd gradient (Fig. 5c).

The recognition of this control challenges a recent interpretation of the Peruvian OMZ δ^{114}Cd–Cd* relationship as evidence for widespread CdS formation (Guinoiseau et al., 2018). In fact, as Fig. S5 shows, the main negative δ^{114}Cd–Cd* correlation in the Peruvian OMZ is identical to the preformed correlation observed in the western subtropical Pacific, and thus provides no evidence for CdS formation. The tropical and subtropical δ^{114}Cd–Cd* relationships do differ in the most O_2-depleted waters, but as a consequence of the *high* OMZ Cd* values produced by biological uptake and export in the upwelling regime. As we discuss in Section 3.6, this Cd-rich biological export also has implications for recent estimates of the contribution of water-column CdS formation to excess Cd in Peruvian shelf and slope sediments.

3.3.3. A Cd sink in the open tropical Pacific?

A final – but key – feature of the Cd distribution along GP16 is the strongly negative Cd* minimum observed within the muted oxygen minimum of the open tropical Pacific (Fig. 5a,b). The distributions of N* and the nitrogen isotope composition of nitrate (δ^{15}N-NO_3) clearly indicate that this oxygen-minimum layer communicates with the zone of active fixed nitrogen loss within the OMZ (Peters et al., 2018). However, while the N* and δ^{15}N-NO_3 signals become weaker away from the OMZ, indicating a mixing-related attenuation, the Cd* minimum is *more* extreme in the open tropical Pacific, and extends to shallower density levels. The Cd* minimum is consistently associated with the oxycline above the O_2 minimum at all open tropical stations, and is centred at a slightly shallower isopycnal, $\gamma^n = 26.5$ kg/m^3, than the O_2 minimum (Figs. 5b and S6). Numerous mechanisms might cause this stronger Cd* minimum: (a) remineralisation at a Cd:P below the *expected mean*; (b) North Pacific influence on the equatorial thermocline; or (c) local/regional Cd loss.

The Cd:P of euphotic-zone particles in the productive equatorial Pacific is highly elevated; for example, the median Cd:P of particles < 51 μm in the equatorial Pacific upwelling (12°S–12°N) is 0.77 mmol/mol (range 0.29–2.0 mmol/mol, $n = 21$; Bourne et al., 2018), and particulate Cd:P is highest (1.18–2.0 mmol/mol, $n = 4$) under more productive upwelling conditions (Bourne et al., 2018). In Supplementary Discussion 1, we argue that this high Cd:P makes it extremely unlikely for remineralisation to reduce Cd*, despite the preferential remineralisation of particulate P in the shallow subsurface (Bourne et al., 2018), the preferential remineralisation of *dissolved* organic phosphorus over the dissolved organic nitrogen that presumably hosts protein-associated Cd (e.g. Letscher and Moore, 2015; Sipler and Bronk, 2015), and uncertainties associated with temporal variability in particle fields. With regard to North Pacific influence, limited dissolved Cd data from the mid-latitude North Pacific shows that the Cd* minimum there (-0.15 nmol/kg by our definition; Conway and John, 2015b; Yang et al., 2018) is less extreme than in the open tropical Pacific.

The fact that neither remineralisation nor North Pacific influence seem likely to produce the open tropical Pacific Cd* minimum indicates that it must be regionally produced, and could result from Cd loss. This possibility receives strong support from the observation that the open tropical Pacific oxycline is consistently associated with *particulate* Cd peaks (Ohnemus et al., 2017; 2019). Indeed, a comparison of dissolved and particulate data (Fig. 6) shows that the Cd* minimum is associated with a particulate Cd maximum at every sampled location in the open tropical Pacific. Size-fractionated particulate data (Lee et al., 2018) reveal that this increase in particulate Cd occurs in both the large and small size fractions. Our recognition of these complementary signals in the particulate and dissolved data strongly suggests that the stronger Cd* minimum in the open tropical Pacific oxycline – outside the O_2-depleted OMZ – is driven by a Cd loss to the particulate phase. Based on their statistical analysis, Ohnemus et al. (2019) attribute the accumulation of particulate Cd to "secondary biomass", which they assume to be heterotrophic and prokaryotic, but further data are required to conclusively identify the processes at work. Certainly, given the low particulate export flux in this region (e.g. Black et al., 2019), it would appear *a priori* more likely that the Cd loss is associated with some suspended particulate phase (which may be deep-living biota), rather than large sinking particles.

Whatever the process associated with this apparent Cd loss, the open tropical Cd* minimum is not associated with any significant change in dissolved δ^{114}Cd (Fig. 5b,c), an observation that, *prima facie*, argues against a (fractionating) loss process. As has been previously argued for the North Pacific (Conway and John, 2015b; Janssen et al., 2017), the absence of a δ^{114}Cd signal may be due to the high [Cd] of the tropical Pacific thermocline (~0.4 nmol/kg at the Cd* minimum). Given the strong upper-ocean δ^{114}Cd gradient and the small isotope effects of sulphide formation (−0.32‰; Guinoiseau et al., 2018) and biological uptake (−0.2‰ to −0.45‰; Abouchami et al., 2011; Sieber et al., 2019a), even a fractionating loss of Cd from these Cd-rich waters is unlikely to result in a resolvable δ^{114}Cd signal: as detailed in Supplementary Discussion 2, Rayleigh distillation predicts a maximum expected δ^{114}Cd increase of only 0.05–0.10‰, while deep-ocean data from GP16 suggest a limit of resolvability of ± 0.10‰ ($2\sigma_{SD}$ for $\gamma^n \geq 27.9$ kg/m^3, excluding 3 hydrothermally-influenced stations). This inference is supported by contrasting δ^{114}Cd behaviour in the Cd-poorer tropical Atlantic (Section 3.4.4).

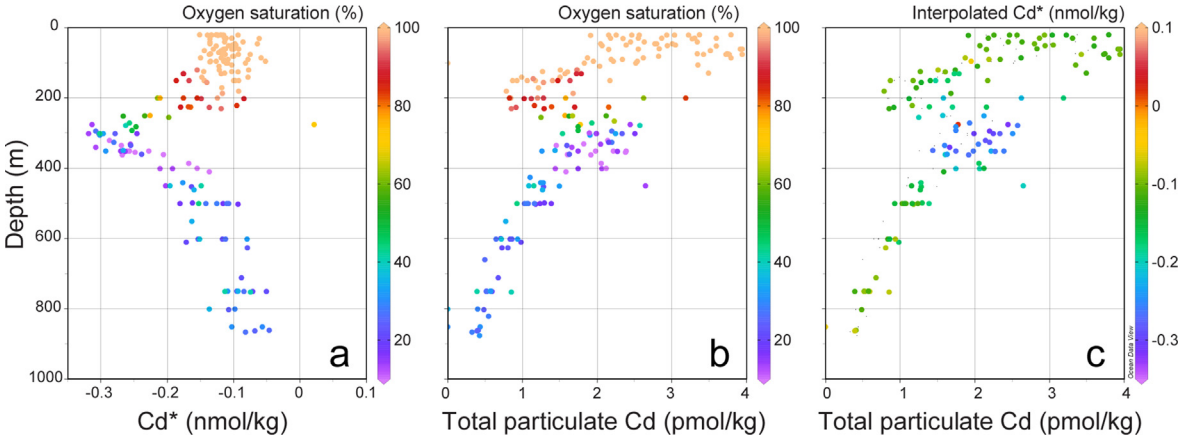

Fig. 6. Spatial relationship between dissolved Cd* minimum and particulate Cd maximum in the open tropical Pacific along GP16 (all stations west of 100°W). (A) Cd* (John et al. 2018) coloured by oxygen saturation from co-analysed O_2 (Schlitzer et al., 2018). (B) Total particulate Cd (Ohnemus et al., 2017) with same colour bar as in panel **a**. (C) Total particulate Cd coloured by Cd* values interpolated linearly from the nearest dissolved Cd data using the interpolation function of Ocean Data View 5 (Schlitzer, 2019).

3.3.4. Summary

This section has demonstrated the importance of remineralisation of Cd-rich organic matter for the Cd distribution in the tropical Pacific, and especially within the Peruvian OMZ. Remineralisation raises Cd* over the entire water column, and especially in the shallow OMZ, where positive Cd* values are observed at the base of the oxycline. A second feature is the strong negative Cd* minimum that is observed above the milder oxygen minimum (50–75 μmol/kg) of the open tropical Pacific, which appears to be related to Cd loss to particulates. The tropical oxycline is thus associated with both an *excess* of Cd (in the OMZ) and a *deficit* (in the central tropics). We consider it possible that the subtle loss process whose consequences are visible in open tropical Cd* is in fact ubiquitous in the tropical oxycline, but that its influence on Cd* within the OMZ is overprinted by the strong signal of remineralisation.

3.4. Atlantic low-latitude cycling

The OMZ systematics of the tropical Pacific are contrasted almost diametrically by those of the tropical Atlantic OMZs. As reported by Janssen et al. (2014) and Conway and John (2015a), the North Atlantic OMZ bears strongly *negative* Cd* values in the shallow subsurface, coinciding with the tropical oxycline; Guinoiseau et al. (2019) have recently shown the same for the South Atlantic OMZ. In the following, we aim to understand the drivers of the differences in the Cd* and δ^{114}Cd distributions between Atlantic and Pacific OMZs. We do so by placing tropical Atlantic observations (Conway and John, 2015a; Guinoiseau et al., 2019; Xie et al., 2019a) in the context of the Cd* and δ^{114}Cd distributions of the well-ventilated western South Atlantic (Fig. 4Xie et al., 2017; Middag et al., 2018). Our inclusion of the North Atlantic OMZ (Conway and John, 2015a) in this framework is based on the recognition that the Cd* anomaly here is hosted in waters of primarily South Atlantic origin (Supplementary Discussion 3), allowing us to consider it together with the southerly-ventilated equatorial Atlantic (Xie et al., 2019a) and South Atlantic OMZ (Guinoiseau et al., 2019).

3.4.1. Subtropical-tropical comparison

Fig. 7 presents isopycnal [Cd], Cd* and δ^{114}Cd distributions in the tropical and southern subtropical Atlantic. The distributions of Cd and PO_4 (Fig. 7a,d) show the combined influence of remineralisation and water mass transport in the Atlantic Ocean. Firstly, the subtropical concentration maximum of nutrient-rich Upper Circumpolar Deep Water ($\gamma^n \sim 27.75$ kg/m^3) is eroded away towards the north by mixing with nutrient-poorer North Atlantic Deep Water, which forms a marked [Cd] and [PO_4] minimum centred around 28 kg/m^3 in the tropical Atlantic. Secondly, low-latitude remineralisation increases [Cd] and [PO_4] in the upper water column of the tropics, and results in a shallow tropical nutrient maximum at $\gamma^n = 27.4$ kg/m^3. The upper-ocean [Cd] increase is much weaker than that of [PO_4] (Fig. 7a,d), reflecting the low Cd:P of remineralisation (Quay et al., 2015; Roshan and Wu, 2015; Middag et al., 2018). In the North Atlantic tropics, concentrations of Cd (but not PO_4) are significantly lower at intermediate depths (γ^n = 27.25–27.75 kg/m^3) than elsewhere in the tropics (Fig. 7a,d), likely due to the influence of Cd-poor and saline North Atlantic water masses (Conway and John, 2015a; Jenkins et al., 2015) visible in the salinity distribution (Fig. 7f).

The distributions of Cd* and δ^{114}Cd (Fig. 7b,c) are much less affected by tropical remineralisation than [Cd], analogous to the South Pacific (Fig. 5b,c; Section 3.3.2). Their distributions are mainly determined by the preformed structure set by the Southern Ocean (Section 3.2) and visible in the southern subtropical data (Fig. 7b,c), i.e. the steady upward increase in δ^{114}Cd, and the Cd* minimum of around −0.2 nmol/kg at the density of Southern Ocean mode waters ($\gamma^n = 26.8$–27 kg/m^3). Nonetheless, remineralisation below the *expected mean* of 0.33 mmol/mol (0.17–0.26 mmol/mol; Quay et al., 2015; Roshan and Wu,

2015; Middag et al., 2018) results in a slight general Cd* decrease in the tropics relative to the subtropics (Fig. 7b), with no apparent effect on the δ^{114}Cd distribution (Fig. 7c). As with the [Cd] distribution, the intermediate North Atlantic (γ^n = 27.25–27.75 kg/m^3) is an exception here, with Cd* ~0.1 nmol/kg lower than other tropical waters, and a hint of slightly elevated δ^{114}Cd values, although offsets at densities > 27 kg/m^3 are only seen at a single station, and are on the order of the inter-laboratory reproducibility (±0.07‰). The most coherent Cd*

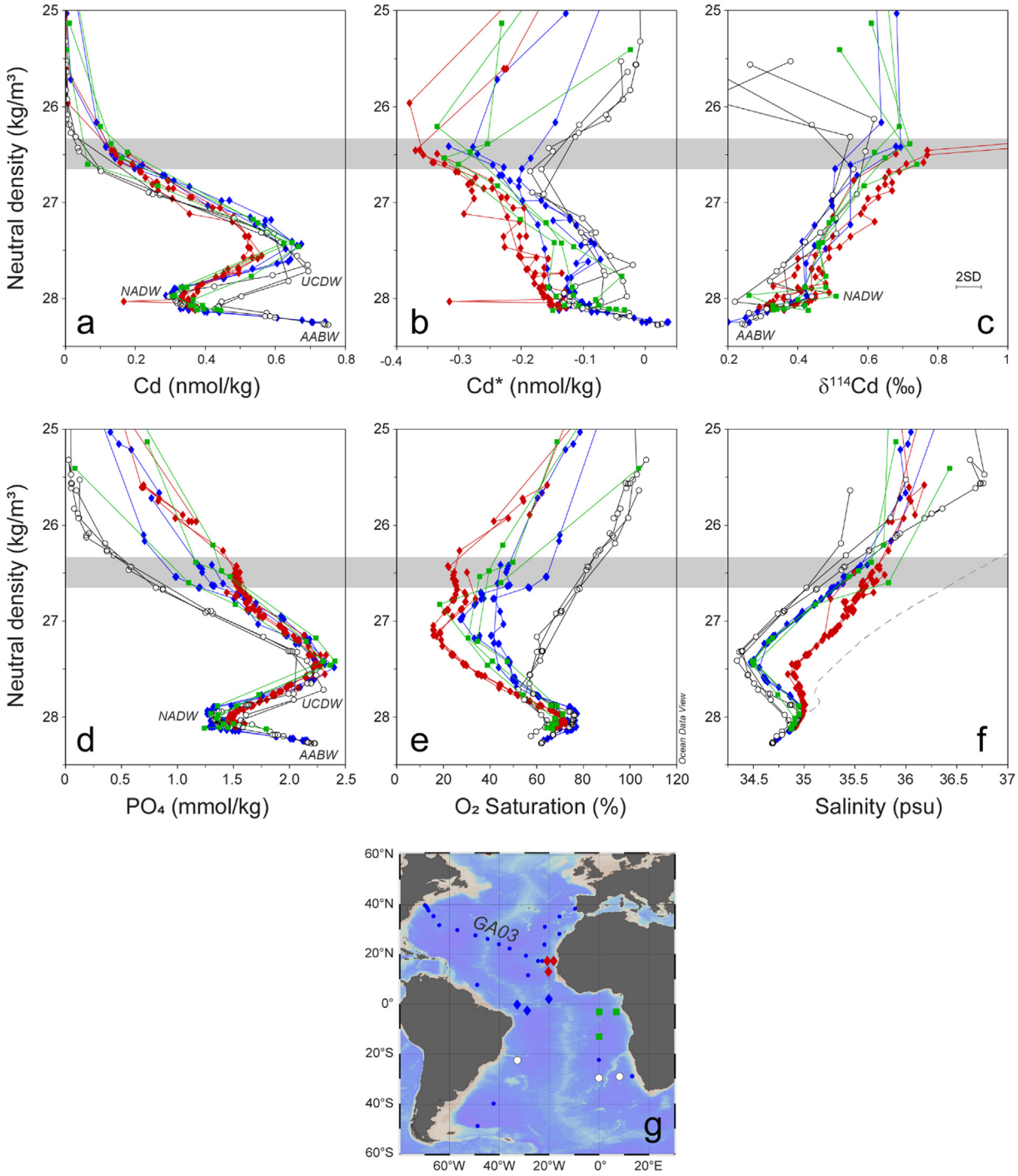

Fig. 7. Subtropical-tropical isopycnal systematics of the Atlantic. White circles: southern subtropics (Xie et al., 2017; Guinoiseau et al., 2019); green squares: South Atlantic OMZ (Guinoiseau et al., 2019); blue squares: equatorial Atlantic (Xie et al., 2019b); red diamonds: North Atlantic OMZ (Conway and John, 2015a; Xie et al., 2019b). Small blue circles denote stations with δ^{114}Cd data that are not shown here. The grey bar marks the density range of the tropical Cd* minimum. Note that Cd* is calculated as defined in Eq. (1), which differs from previous applications of Cd* to the Atlantic Ocean, including in the works cited above.

difference between the tropics and the southern subtropics is the stronger tropical Cd* minimum in the upper thermocline, at $\gamma^n \approx 26.5$ kg/m^3 (grey band in Fig. 7). This stronger Cd* minimum is visible in the western equatorial Atlantic, and becomes more negative in the North and South Atlantic OMZs (Fig. 7b), where [PO_4] is higher (Fig. 7d) but [Cd] barely increases relative to the equatorial Atlantic (Fig. 7a). These Cd* minima are associated with the tropical oxycline (Fig. 7e; Conway and John, 2015a; Guinoiseau et al., 2019), as observed in the *open* tropical Pacific along GEOTRACES section GP16 (Section 3.3; Fig. 6). However, the shallow OMZ Cd* minima of the Atlantic contrast strongly with the Cd* *maximum* observed at the oxycline above the OMZ of the tropical South Pacific (Fig. 5b).

3.4.2. Influence of low-latitude remineralisation on Cd*

Two sets of major-element isotope data from the North Atlantic OMZ indicate that remineralisation drives the difference in OMZ Cd* systematics between the Atlantic and the Pacific (Fig. S7). Firstly, the shallow subsurface Cd* minima of the North Atlantic OMZ (at 51–89 m water depth) coincide with shallow minima in $\delta^{13}C_{DIC}$ (Quay and Wu, 2015), in sharp contrast to the coincidence of Cd* *maxima* with $\delta^{13}C_{DIC}$ minima in the Peruvian OMZ (Fig. 5). Secondly, the North Atlantic Cd* minima also coincide with minima in $\delta^{15}N{-}NO_3$, which unambiguously document the regional regeneration of organic matter bearing low $\delta^{15}N{-}NO_3$ due to nitrogen fixation in the North Atlantic (Marconi et al., 2015). These isotopic and Cd* minima are all hosted within a shallow subsurface O_2 minimum at around 100 m depth ($\gamma^n = 26.5$ kg/m^3) that is physically separate from the deeper, O_2-poorer minimum at 400 m ($\gamma^n = 27$ kg/m^3; Fig. S7). Together, these observations indicate an upwelling-associated remineralisation signal at the level of the shallow Cd* minimum in the North Atlantic OMZ, and likely elsewhere in the tropical Atlantic as well, although co-located $\delta^{13}C_{DIC}$ and $\delta^{15}N{-}NO_3$ are not available.

What is the likely effect of this remineralisation on Atlantic Cd*? Limited particulate data from above the North Atlantic OMZ indicate a mean euphotic-zone particulate Cd:P of 0.36 mmol/mol ($n = 3$; Bourne et al., 2018), much lower than Cd:P > 1 mmol/mol above the Peruvian OMZ (Bourne et al., 2018), and similar to the *expected mean* of 0.33 mmol/mol. The scant Atlantic data and significant seasonal Cd:P variability observed elsewhere in the ocean (Bourne et al., 2018) result in some uncertainty here, but bulk particle remineralisation at the observed Cd:P ratios would not be expected to lower Cd* in the North Atlantic OMZ. Following our discussion in Supplementary Discussion 1, it is likely that the preferential shallow remineralisation of P over Cd (Bourne et al., 2018; Cloete et al., 2021) will result in a Cd:P signal from remineralisation that is lower than bulk particle Cd:P in the very shallow subsurface. This reduction is difficult to quantify, but regardless of its extent, the existing particulate Cd:P data suggest that remineralisation is unlikely to *raise* Cd* in the shallow North Atlantic OMZ – in strong contrast to the Peruvian OMZ (Section 3.3.2; Fig. 5). Together with the well-documented low Cd:P of Atlantic remineralisation inferred from independent dissolved data (Quay et al., 2015; Roshan and Wu, 2015; Middag et al., 2018; Roshan and DeVries, 2021), this leads us to postulate that the tendency of remineralisation to either lower or not alter Cd* applies to the entire tropical Atlantic.

Thus, one reason for the difference in the Cd* systematics between the South Pacific and Atlantic OMZs may be the fact that, while remineralisation will certainly raise Cd* in Pacific OMZs, it does not seem to in the Atlantic. Given this near-neutral influence of remineralisation on Atlantic Cd*, the upper-OMZ Cd* distribution may be influenced, in near-coastal waters, by excess PO_4 released from anoxic shelf sediments at depths close to the Cd* minimum (Schroller-Lomnitz et al., 2019). Benthic PO_4 fluxes are mechanistically coupled to those of Fe (e.g. Ingall and Jahnke, 1994; Noffke et al., 2012), and dissolved Fe stable isotopes (Conway and John, 2014; Klar et al., 2018) fingerprint sedimentary release of reduced Fe to the shallow North Atlantic OMZ waters that host the Cd* minimum. Together, the recognition of remineralisation and potential benthic flux signals in these waters suggests that the evidence in the North Atlantic OMZ Cd* distribution for widespread particle-hosted CdS formation is more ambiguous than has previously been inferred (see also Section 3.6; Janssen et al., 2014; Conway and John, 2015a).

3.4.3. A Cd sink in the tropical Atlantic?

However, there is also the evidence of the δ^{114}Cd distribution to consider. As in the South Pacific (Fig. 5), the isopycnal structure of tropical Atlantic δ^{114}Cd is largely set by the preformed distribution visible in the subtropical South Atlantic (Fig. 4; Fig. 7c; Xie et al., 2017). However, at upper thermocline depths hosting the tropical Cd* minimum, δ^{114}Cd values are consistently higher than in the subtropics (Fig. 7c). The isopycnal δ^{114}Cd offset from southern subtropical waters averages 0.1‰ ($n = 7$) and ranges from 0.03–0.18‰, with the largest offsets observed in the North Atlantic (Fig. 7c). We acknowledge that southern subtropical data around this density range are limited, and the δ^{114}Cd differences are small relative to the inter-laboratory reproducibility of ± 0.07‰. However, most of the Atlantic data (with the exception of the North Atlantic) were analysed in a single laboratory (Xie et al., 2017; Guinoiseau et al., 2019; Xie et al., 2019a) with a better external reproducibility of ± 0.04–0.05‰ (Guinoiseau et al., 2019). Thus, considering that marine δ^{114}Cd profiles exhibit consistency within oceanographic regions (e.g. Yang et al., 2018; George et al., 2019; Sieber et al., 2019b), the consistent association of higher δ^{114}Cd values with the tropical Cd* minimum (Fig. 7b,c) suggests a true elevation of δ^{114}Cd in the upper tropical Atlantic thermocline relative to the subtropics. While this observation requires confirmation by future analyses, it receives support from the fact that many of the δ^{114}Cd values observed in the Cd* minimum are as high as, or higher than, the values in the overlying surface waters (an obvious exception are the North Atlantic data, but the fidelity of the high δ^{114}Cd values in overlying waters here remains debated; e.g. Xie et al., 2017; Guinoiseau et al., 2019; Sieber et al., 2019b).

Together, the stronger Cd* minimum and elevated δ^{114}Cd in the tropical Atlantic oxycline seem to indicate a Cd loss process here. Crucially, however, this potential loss signal is visible not only in the OMZs, but also within better-ventilated tropical waters of the western equatorial Atlantic (Fig. 7b,c,e; Xie et al., 2019a). This suggests that the loss process reflected in Cd* and δ^{114}Cd is not specific to OMZ waters, but may in fact be a general feature of the tropical Atlantic oxycline – analogous to the stronger Cd* minimum observed in the oxycline of the open tropical Pacific (Section 3.3.3). This inference receives support from data across the western subtropical and tropical Atlantic (Middag et al., 2018) showing that a stronger Cd* minimum, associated with the tropical oxycline, appears at the transition from the southern subtropics to the tropics (Fig. S8). This tropical Atlantic Cd* minimum is slightly shallower than the O_2 minimum, as in the South Pacific (Fig. S6), and shoals isopycnally towards the equator (Fig. S8). Fig. 8 shows that at comparable latitudes, the shallow tropical Atlantic Cd* distribution is near-identical to that of the open tropical Pacific (Fig. 8a,b), despite higher O_2 saturation in the better-ventilated Atlantic (Fig. 8c,d). As discussed in Section 3.3.3, the open tropical Pacific Cd* minimum is *consistently* associated with a subsurface particulate Cd maximum (Fig. 6; Ohnemus et al., 2019), indicating a Cd loss there. No co-sampled particulate Cd data are available for the Atlantic, but here we instead have the evidence of the δ^{114}Cd distribution (Fig. 7c), which suggests a fractionating Cd loss process associated with the tropical Cd* minimum.

Thus, two independent lines of evidence, from two different oceans, appear to provide support for Cd loss in the shallow tropical oxycline. This inference is consistent with the limited data available for the Indian Ocean (Vu and Sohrin, 2013) which, though not complemented by isotopic or particulate data, show the subtropical preformed Cd* minimum giving way to a shallow tropical minimum at $\sim$ 100 m depth (Fig. S9). Furthermore, the presence of a resolvable δ^{114}Cd signal in the Atlantic (Fig. 7c), but not in the Pacific (Fig. 5c), is entirely consistent with the same loss process operating in both oceans. Our calculations in Supplementary Discussion 2 indicate that while Cd loss from the Cd-rich tropical Pacific would not produce a resolvable δ^{114}Cd elevation at the Cd* minimum, the same Cd* decrease in the nutrient-poorer Atlantic would increase δ^{114}Cd by 0.11–0.26‰, entirely in keeping with the observations (Fig. 7c). Thus, although the tropical Atlantic Cd*–δ^{114}Cd correlation primarily results from the preformed distribution rather than Cd loss (as in the Pacific; Fig. S5), tropical Cd loss does extend this correlation to slightly more extreme values than in the southern subtropics (Fig. S10; Conway and John, 2015a; Xie et al., 2019a; Guinoiseau et al., 2019). However, this signal is not restricted to O_2-poor OMZ waters, but is visible throughout the Atlantic tropics (Figs. 8, S8). Furthermore, the δ^{114}Cd shift is too small for it to be diagnostic of any one process such as sulphide formation or biological uptake.

3.5. Synthesis: Cd systematics in the low-latitude Pacific and Atlantic

We have shown that the covariation of Cd* and δ^{114}Cd observed in low-latitude OMZs of the Atlantic and Pacific comes about primarily due to the coupling of Cd* and δ^{114}Cd by phytoplankton uptake in the Southern Ocean, and not because of CdS precipitation. Nonetheless, particulate elemental and limited dissolved isotopic data appear to support the existence of a Cd loss process that creates a stronger Cd* minimum in the tropical oxycline of the Pacific and Atlantic (Sections 3.3 and 3.4). However, this process is not limited to eastern-boundary OMZs, as has been previously proposed (Janssen et al., 2014; Conway and John, 2015a; Janssen et al., 2017; Guinoiseau et al., 2019), but instead seems to extend throughout the tropics (Figs. S8 and S9). We suggest that the influence of this loss process is masked in the Peruvian OMZ by the remineralisation of Cd-rich biogenic particles (Section 3.3.2; Black et al., 2019), while in the Atlantic OMZs, the lower Cd:P ratio of sinking particles (Bourne et al., 2018) either exacerbates the reduction in Cd* or plays a neutral role (Section 3.4.2). The difference in the Cd* systematics between the Atlantic and South Pacific OMZs can thus be largely explained by differences in the Cd:P stoichiometry of exported particles. Below, we consider the drivers and consequences of this difference (Section 3.5.1) before discussing possible mechanisms of Cd loss in the tropical oxycline and identifying questions to be addressed by future research (Section 3.5.2).

3.5.1. Particulate Cd:P systematics and their influence on the Cd distribution

Euphotic-zone particulate Cd:P ratios reach much higher values (up to 1.42 mmol/mol) in the upwelling region above the South Pacific OMZ than above the North Atlantic OMZ (up to 0.36 mmol/mol; Bourne et al., 2018). These data are from GEOTRACES sections that extend from upwelling regions into the open oligotrophic tropics (GP16) or subtropics (GA03), where euphotic-zone particulate Cd:P ratios are low, with median values of 0.21 mmol/mol ($n = 11$) and 0.09 mmol/mol ($n = 8$) respectively (Bourne et al., 2018). Fig. 9 compiles these euphotic-zone particulate compositions with euphotic-zone average dissolved [Cd] from seawaters sampled on the same cruises, calculated from IDP2017v2 data (Schlitzer et al., 2018). Given the simplicity of this comparison and the complexity of the phytoplankton ecosystem changes between upwelling regions and the oligotrophic ocean, Fig. 9 reveals an astonishingly coherent relationship between [Cd] and particulate Cd:P. In general, particulate Cd:P increases with [Cd], with a non-linear dependence that can be statistically described as either logarithmic or following saturating Michaelis-Menten dynamics (curves in Fig. 9a,b). However, the relationship is most systematic at low [Cd], below $\sim$ 10 pmol/kg in both oceans (Fig. 9c); at higher [Cd] there is significant scatter. While culturing studies have shown an increase in eukaryotic Cd quota with dissolved *inorganic* Cd (Lee

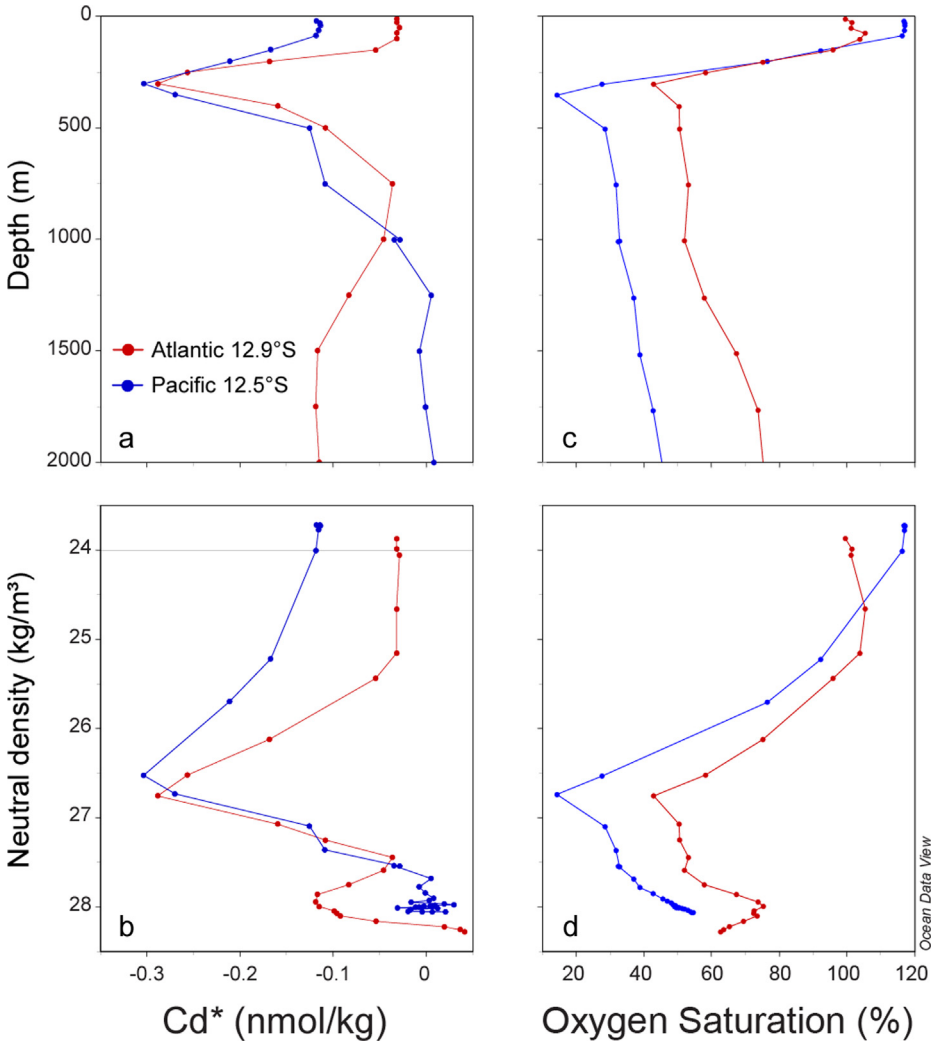

Fig. 8. Similarity between (A, C) Cd* and (B, D) O2 saturation distributions at comparable latitudes in the tropical South Pacific (GP16 Sta. 25) and South Atlantic (GA02 Leg 3, Sta. 14). This similarity holds for all open tropical stations (west of 100°W) on GP16. Data are from John et al. (2018a), Middag et al. (2018) and Schlitzer et al. (2018).

et al., 1995; Sunda and Huntsman, 1998, 2000), limited observations indicate that ~ 70% of Cd is organically chelated in the subtropical surface (Bruland, 1992). The systematic relationship between particulate Cd:P and [Cd] in the oligotrophic waters may thus reflect relatively constant concentrations of Cd-chelating ligands, especially in the North Atlantic subtropics where euphotic-zone Cd:P and [Cd] are tightly coupled (Fig. 9b,c).

More generally, the oligotrophic systematics suggest that phytoplankton take up more Cd as its dissolved concentration increases, perhaps due to the non-specificity of divalent metal transporters, or targeted Cd uptake at the low dissolved [Zn] of the low-latitude ocean (Sunda and Huntsman, 2000; Lane et al., 2009). At higher [Cd], both the shift towards higher particulate Cd:P as well as the larger scatter most likely result from ecosystem shifts between oligotrophic and upwelling-influenced regimes, since (a) there are clear group-level differences in phytoplankton Cd quota (Lane et al., 2009), and (b) within upwelling-influenced regimes, phytoplankton community structure shifts towards larger eukaryotes (e.g. Franz et al., 2012) with elevated Cd quotas (Twining and Baines, 2013), as reflected by higher particulate Cd:P in the equatorial Pacific during upwelling conditions (Bourne et al., 2018). However, most broadly, the factor ~ 4 higher particulate Cd:P observed in the South Pacific is associated with euphotic-zone [Cd] an order of magnitude higher than in the North Atlantic (Fig. 9a,b,c). Similar covariation between co-sampled euphotic-zone [Cd] and particulate Cd:P has recently been observed in the Southern Ocean (Cloete et al., 2021). Thus, while inter-basin differences in species and ecosystem structure as well as (micro)nutrient status (Sunda and Huntsman, 1998, 2000; Cullen et al., 2003; Lane et al., 2009; Bourne et al., 2018) likely play some role in determining the difference in particulate Cd:P between the Atlantic and Pacific, it appears that the difference in [Cd] in these two upwelling regions is a first-order driver of differences in particulate Cd:P stoichiometry.

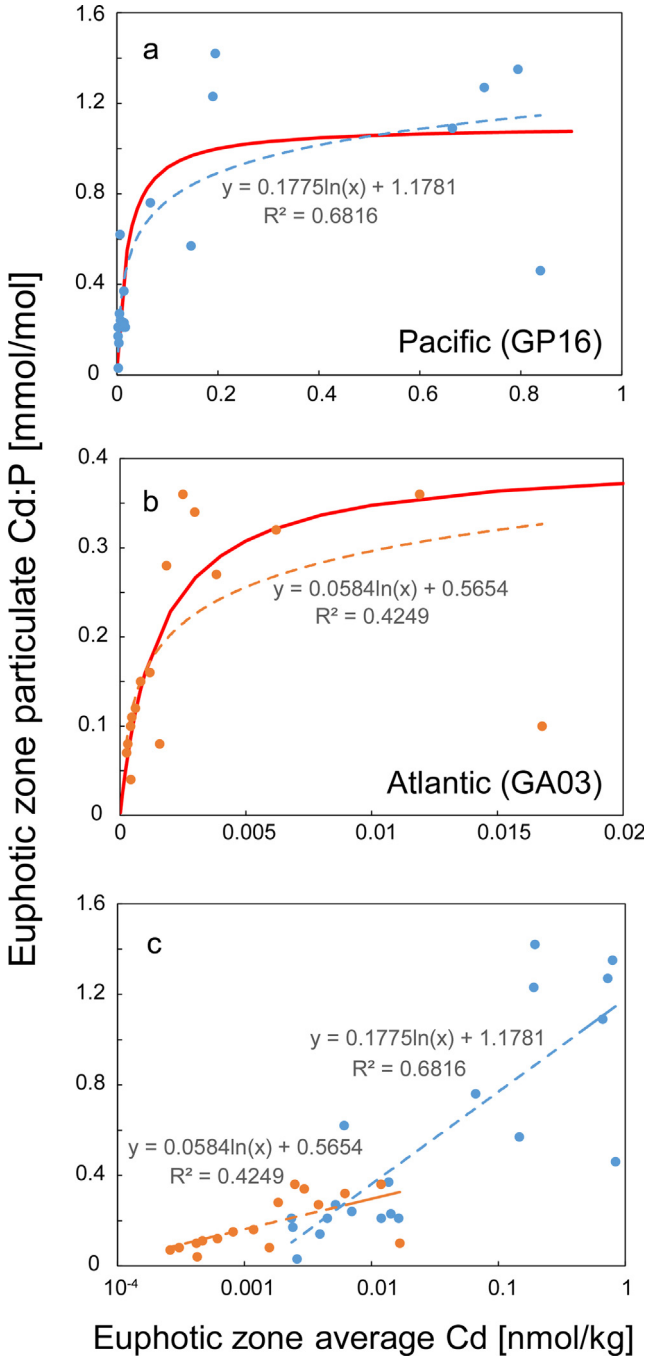

Fig. 9. Cd:P systematics of euphotic-zone particulates along (**A**) Pacific section GP16 and (**B**) Atlantic section GA03. Dashed lines are logarithmic fits (with equations), red lines are Michaelis-Menten curves. (**C**) Compares data from both cruises on a logarithmic *x*-axis. Particulate data from Bourne et al. (2018), dissolved data from Schlitzer et al. (2018). Dissolved data were averaged over euphotic-zone depths reported by Bourne et al. (2018).

The inference of a [Cd] control on particulate Cd:P in the *low* latitudes of the Atlantic and Pacific is directly analogous to Middag et al.'s (2018) invocation of a [Cd] control to explain differences in the Cd:P of export between the *high* latitudes of the Southern Ocean and subarctic North Atlantic. Indeed, biological Cd:P plasticity may be by far the most important process shaping the global-scale marine Cd (and Cd*) distribution. As has been previously argued (Saager and de Baar, 1993; Sunda and Huntsman, 2000; Cullen et al., 2003; Baars et al., 2014; Quay et al., 2015; Xie et al., 2015; Roshan et al., 2017; Roshan and DeVries, 2021) the high Cd:PO_4 uptake of Southern Ocean phytoplankton decouples the global Cd and PO_4 distributions, through its influence on preformed Cd and PO_4. This preformed structure is primarily modified by low-latitude productivity in the tropics, where export fluxes are high.

Here, biological Cd:P plasticity plays a role once again: in the Cd-poor tropical Atlantic, the remineralisation of particles with low Cd:P (Twining et al., 2015; Bourne et al., 2018; Middag et al., 2018) tends to lower Cd* in the interior (Roshan and DeVries, 2021); while in the Cd-richer Pacific, exported particulates generally have higher Cd:P (Bourne et al., 2018; Black et al., 2019) and tend to raise Cd*, especially below upwelling regions where ample Cd is supplied to surface ecosystems. Thus, variability in the Cd:P of biological uptake and export at both high and low latitudes, potentially driven by [Cd], will tend to decouple the Cd and PO_4 distributions, producing signals in the interior Cd* distribution that – though solely reflecting biological cycling – may mimic Cd loss.

3.5.2. Mechanisms driving tropical Cd loss

Identifying the process that drives the putative Cd loss we identify in the tropical oxycline is exceedingly difficult based on available data. What is clear is that the Cd* minimum is associated with particulate Cd maxima in the open tropical Pacific (Fig. 6; Ohnemus et al., 2019) as well as the North Atlantic OMZ (Conway and John, 2015a). Ohnemus et al. (2019) attributed the open tropical Pacific particulate maxima to the presence of heterotrophic prokaryotes, while Janssen et al. (2014) and Conway and John (2015a) attributed the North Atlantic maxima to CdS precipitation within decomposing particles. In the anoxic Peruvian OMZ, where active sulphur cycling is known to occur (Canfield et al., 2010), Ohnemus et al. (2017) argue that the stoichiometric ratio of ≤ 1 mol:mol observed between particulate Cd and acid-volatile sulphides is consistent with, but not convincing evidence for, a sulphide carrier of particulate Cd there. However, continued cryptic sulphur cycling in the O_2-richer oxygen minima (50–150 μmol/kg) of the wider tropical Atlantic and Pacific is highly unlikely. Furthermore, the Cd* minimum with its associated particulate Cd maximum is observed even in oligotrophic regions, where sinking particulate fluxes are low (Honjo et al., 2008). Given the apparent dependence of particle-hosted sulphate reduction on productivity (Raven et al., 2021), it appears that CdS precipitation within the sulphidic cores of large sinking particles, as proposed by Janssen et al. (2014) and simulated by Bianchi et al. (2018), cannot be invoked as an explanation for the shallow Cd* minimum associated with the oxycline *throughout* the tropics.

On the other hand, the attribution of the open tropical Pacific particulate Cd maxima to heterotrophic prokaryotes is based on statistical analysis of particulate chemistry data (Ohnemus et al., 2019), and remains to be confirmed through more detailed particle characterisation. Although speculative, it is worth noting that the tropical Cd* minima are sometimes shallow enough to overlap with elevated fluorescence in the tail of the deep chlorophyll maximum (e.g. Fig. S11). Genetic data indicate the presence of low-light-adapted ecotypes of the ubiquitous low-latitude cyanobacterial phytoplankton *Prochlorococcus* at depths of $\sim$ 100 m throughout the tropical Atlantic (Johnson et al., 2006) and in the Peruvian OMZ (Franz et al., 2012), i.e. within the depth range of the Cd* minimum in regions of upwelling-related isopycnal uplift. This raises the possibility that *autotrophic* prokaryotic shade flora may have a role to play in tropical Cd loss (Ohnemus et al., 2017), at least at shallower levels within the euphotic zone. While prokaryotic phytoplankton generally take up only small amounts of chalcophilic metals like Cd (e.g. Saito et al., 2003), laboratory cultures have shown that under low light, the Cd:P of a cyanobacterial species (*Cyanothece* sp.) increases to ratios similar to those of eukaryotes (Finkel et al., 2007). It is unknown whether this result translates to *Prochlorococcus*, or whether it would apply to low-light-adapted ecotypes. However, in the subtropical North Atlantic, Twining et al. (2015) also report higher labile particulate Cd:P ratios in the deep chlorophyll maximum than in the mixed layer. Clearly, we are at an early stage of understanding tropical Cd loss mechanisms, and future work that enables the simultaneous characterisation of microbial ecosystem functioning (e.g. through 'omics approaches or analysis of environmental DNA; e.g. Ruppert et al., 2019; Debeljak et al., 2021), of dissolved phase behaviour, and of particulate hosting phases, will be required to conclusively identify the driving process(es).

3.6. Implications for marine Cd mass balance

Our investigation of the ocean-internal cycling of Cd has two sets of implications for the role of water-column CdS formation in the marine Cd budget. But first, we must distinguish between two marine CdS formation regimes. One regime exists within functionally anoxic OMZs, in which H_2S may be present in the water column in trace to micromolar amounts. For example, Plass et al. (2020) have documented Cd loss from bottom waters above sulphidic sediments on the Peruvian shelf (0.4–9.5 μM H_2S in near-surface porewater). This observation, presumed to result from CdS precipitation in the presence of trace H_2S, is consistent with previous observations of Cd loss associated with episodic H_2S release into the water column here (Schunck et al., 2013; Xie et al., 2019b) and, more generally, with enhanced accumulation of Cd in upwelling-margin and euxinic-basin sediments (Little et al., 2015; Chen et al., 2021). The second regime involves CdS precipitation in sulphidic microenvironments within sinking particles (Janssen et al., 2014), and it is this regime to which our discussion is directly pertinent.

Plass et al. (2020) estimate that CdS precipitation (either in near-bottom waters or via shallower particle-associated processes) supplies a minimum of 28–67% of excess Cd in the sediments they studied – including in non-sulphidic sediments situated in oxygenated waters below the depth of the Peruvian OMZ (750 m water depth, >5 μM bottom-water O_2). A major supply of CdS to non-sulphidic sediment suggests a rain of particle-hosted CdS formed at the upper oxycline (Janssen et al., 2014), 700 m above the seafloor. However, Plass et al.'s (2020) CdS flux estimate hinges critically on the estimated supply of Cd from biogenic particles, calculated by scaling organic carbon (C) fluxes with an "average phytoplankton" Cd:C of 1.69 μmol/mol (Moore et al., 2013). This value, derived from a Cd:P of 0.21 mmol/mol (Ho et al., 2003), stands in stark contrast to the Cd:P of $\sim$ 0.95 mmol/mol in euphotic-zone particles

(Bourne et al., 2018) and the export flux (Black et al., 2019) over the Peruvian shelf. Recalculation using this site-specific stoichiometry suggests that biogenic particles can in fact easily account for all excess Cd found in non-sulphidic sediment deeper than the OMZ (Table S1). Thus, there is little need to invoke a sulphide carrier of Cd to non-sulphidic sediments of the Peruvian margin.

Two complexities must however be noted with regard to our recalculation. The first is that particulate fields vary temporally and spatially; e.g., the Cd:P of export over the Peruvian shelf and slope varies from 0.52 mmol/mol to 1.11 mmol/mol (Black et al., 2019; Table S2), variability that propagates into our calculations (Table S1). Secondly, particulate Cd:P is not conserved through the water column: differential remineralisation decreases Cd:P with depth (Bourne et al., 2018; Cloete et al., 2021), while within the OMZ, particulate Cd:P may increase due to prokaryotic trace metal accumulation (Ohnemus et al., 2017) or Cd adsorption (Lee et al., 2018). How strongly such secondary processes affect the Cd:P of the *sinking* flux is difficult to quantify, but they will certainly have a larger effect over the deeper water column above the non-sulphidic slope sediments than on the shelf. Large particle (>51 μm) data from the Peruvian OMZ suggest that Cd:P decreases by ~ 50% between 50 m and 500 m (Lee et al., 2018), perhaps explaining why the Cd:P of export (Black et al., 2019) can explain up to ~ 4 times the excess Cd in slope sediments (Table S1).

Most broadly, however, our inference that no CdS carrier is needed to explain excess Cd in non-sulphidic sediments of the Peruvian margin is consistent with observations in similar sediments in the South Atlantic (Bryan et al., 2021). A major biological contribution to excess Cd in Peru margin sediments is also in line with the finding by Chen et al. (2021) that organic matter can account for 50–100% of excess Cd in analogous sediments of the eastern tropical North Pacific. Furthermore, the fact that the low "average phytoplankton" Cd:P of 0.21 mmol/mol can explain excess sedimentary Cd in the Cd-poor Atlantic (Bryan et al., 2021) but not the Pacific (Plass et al., 2020) is consistent with the systematics of Fig. 9 as well as the inter-basin differences in particulate Cd:P observed directly (e.g. Bourne et al., 2018) or inferred from water-column data (Quay et al., 2015; Roshan and DeVries, 2021). These observations highlight the importance of considering biological metal-quota plasticity in sedimentary studies, as has recently been recognised for Cd and other metals (Chen et al., 2021; Plass et al., 2021).

The fact that there is no need to invoke a sulphide carrier of Cd to sediments deeper than OMZ extent, when combined with the potential biological mechanism of particulate Cd accumulation within tropical OMZs (Ohnemus et al., 2017), has implications for a recent estimate of particle-hosted CdS formation (Bianchi et al., 2018) and the associated marine Cd sink (Guinoiseau et al., 2019). The parameters of Bianchi et al.'s (2018) particle model, such as the rate constants for CdS formation and dissolution, were optimised against a particulate Cd profile from the North Atlantic OMZ (Janssen et al., 2014), and converged to a dissolution rate constant 1.5–3 3× higher than experimental or theoretical values, as noted by Guinoiseau et al. (2019). This high value suggests either that marine CdS is more labile than CdS of other origins in other media, or that the optimisation required a high dissolution rate to rapidly attenuate an overestimated CdS pool – perhaps because some portion of the observed particulate Cd is actually due to prokaryotic Cd uptake (Ohnemus et al., 2017). Each of these possibilities suggests that particle-hosted CdS formation will lead to only a small net loss of marine Cd to sediment. Indeed, calculating an internally-consistent estimate of the net CdS sink resulting from the CdS formation flux estimated by Bianchi et al. (2018) yields a value of 25 mol/yr – 1.8×10^7mol/yr (Table S3). These estimates range from entirely negligible for the marine Cd budget to the magnitude of other estimates of Cd loss to suboxic or anoxic sediments ($1.5–12.0 \times 10^7$ mol/yr; Bryan et al., 2021; Chen et al., 2021). Thus while it may be non-negligible, the net loss of Cd associated with particle-hosted CdS formation is unlikely to be the dominant Cd sink in the modern ocean, and is at most at the lower end of the range estimated by Guinoiseau et al. (2019). While there is no simple connection between the two, this inference is in keeping with our analysis in Sections 3.2–3.4, which shows that dissolved data previously interpreted as documenting widespread particle-hosted CdS formation in fact mainly reflect large-scale controls on the Cd distribution, with only a minor role for low-latitude loss processes.

4. CONCLUSIONS

Correlations between Cd* and δ^{114}Cd previously interpreted as evidence for widespread particle-hosted CdS precipitation in OMZs in fact primarily reflect the biologically-controlled preformed distributions of these tracers. Indeed, given such oceanographic structure in their distributions, non-dimensional cross-plots of Cd* against δ^{114}Cd have little value for process identification. We have also shown that remineralisation of biogenic particles, and specifically the large range in their Cd:P stoichiometry, is the most important modifier of the preformed distributions of Cd and Cd* (its influence on δ^{114}Cd is very limited). In particulate elemental and dissolved isotopic data, we find subtle evidence for Cd loss from the oxyclines of the tropical Pacific and Atlantic. An assessment of the global extent of this signal, and its origin, would be aided by higher-resolution dissolved Cd data from the tropical Indian Ocean or the eastern tropical North Pacific OMZ, especially if complemented by particulate and/or isotopic Cd data. Although the process(es) driving this loss remains unclear given the data currently available, it is conceivable that it is biological in origin (Ohnemus et al., 2017; 2019). Regardless of its driving mechanism, the data indicate that Cd loss is ubiquitous in the tropical oxycline, and not confined to the oxygen-poor or -depleted waters of the eastern basins. This realisation implies that the evidence of OMZ particulate Cd data for particle-hosted CdS precipitation is more ambiguous than previously recognised (Janssen et al., 2014; Conway and John, 2015a).

Global extrapolations of these data in order to estimate the magnitude of the water-column CdS sink (Bianchi et al.

2018) and its importance for the marine Cd budget (Guinoiseau et al., 2019) may have overestimated the influence of particle-hosted CdS formation. Furthermore, by considering the extreme Cd:P plasticity in phytoplankton, we show that even in the anoxic Peruvian OMZ underlain by sulphidic sediments that scavenge bottom-water Cd as CdS, Cd supply to the sediment by sinking biogenic particles may contribute significantly (15–90%) to sedimentary Cd, consistent with recent findings in Atlantic and Pacific sediments (Bryan et al., 2021; Chen et al., 2021). Together, this evidence indicates a small or negligible role for particle-hosted sulphide formation in the marine mass balance of Cd.

Declaration of Competing Interest

The authors declare that they have no known competing financial interests or personal relationships that could have appeared to influence the work reported in this paper.

ACKNOWLEDGEMENTS

The authors thank the many scientists and technicians whose analytical work went into the production of the data used in this contribution; the sailors, technicians, student helpers and scientists who made sample acquisition possible; and the GEOTRACES programme for the production of the Intermediate Data Product 2017v2. Paul Quay kindly allowed us to use his Pacific $\delta^{13}C_{DIC}$ data in the GEOTRACES IDP2017v2, and Mathieu Waeles generously shared his Angola Basin data. We thank Reiner Schlitzer for development of Ocean Data View 5 (Schlitzer, 2019) which aided exploratory data analysis and preparation of figures. Careful and constructive reviews by Ruifang Xie, Damien Guinoiseau and two anonymous reviewers, and the editorial oversight of Claudine Stirling, helped to improve the manuscript. This research was supported by ETH Zurich and did not receive any specific grant from funding agencies in the public, commercial, or not-for-profit sectors. SHL is currently supported by a NERC independent research fellowship (NE/P018181/2).

AUTHOR CONTRIBUTIONS

GFdS conceived the study together with MS, TMC and DV, undertook the data analysis, and wrote the first draft. SHL contributed especially to Section 3.6; DV contributed especially to development of the manuscript. All co-authors contributed to the development of the manuscript in preparation for submission.

DATA STATEMENT

The data considered in this study have been previously published by other workers, and almost all are freely available. Most data are to be found in the GEOTRACES Intermediate Data Product 2017v2 at https://www.bodc.ac.uk/geotraces/data/idp2017/ or the GEOTRACES Intermediate Data Product 2021 at https://www.bodc.ac.uk/geotraces/data/dp/. Data from Guinoiseau et al. (2019) are freely available at https://dx.doi.org/10.1029/2019GB006323, the North Pacific data of Yang et al. (2018) are available at https://dx.doi.org/10.1016/j.gca.2018.05.001 (subscription required), and the data of Sieber et al. (2019a,b) are available at https://dx.doi.org/10.1016/j.epsl.2019.115799 and https://dx.doi.org/10.1016/j.chemgeo.2018.07.021 (subscription required). Chlorophyll-*a* data presented in Fig. S11 are publicly available and were downloaded from the British Oceanographic Data Centre (https://www.bodc.ac.uk); they are supplied by the National Environmental Research Council and licenced under the Open Government Licence v1.0.

APPENDIX A. SUPPLEMENTARY DATA

Supplementary data to this article can be found online at https://doi.org/10.1016/j.gca.2022.02.009.

REFERENCES

Abouchami W., Galer S. J. G., de Baar H. J. W., Alderkamp A.-C., Middag R., Laan P. and Andreae M. O. (2011) Modulation of Southern Ocean cadmium isotope signature by ocean circulation and primary productivity. *Earth Planet. Sci. Lett.* **305**, 83–91.

Abouchami W., Galer S. J. G., de Baar H. J. W., Middag R., Vance D., Zhao Y. and Andreae M. O. (2014) Biogeochemical cycling of cadmium isotopes in the Southern Ocean along the Zero Meridian. *Geochim. Cosmochim. Acta* **127**, 348–367.

Baars O., Abouchami W., Galer S. J. G., Boye M. and Croot P. L. (2014) Dissolved cadmium in the Southern Ocean: distribution, speciation, and relation to phosphate. *Limnol. Oceanogr.* **59**, 385–399.

Bianchi D., Weber T. S., Kiko R. and Deutsch C. (2018) Global niche of marine anaerobic metabolisms expanded by particle microenvironments. *Nat. Geosci.* **11**, 263–268.

Black E., Lam P. J., Lee J.-M. and Buesseler K. O. (2019) Insights from the ^{238}U–^{234}Th method into the coupling of biological export and the cycling of cadmium, cobalt and manganese in the southeast Pacific Ocean. *Global Biogeochem. Cycles* **33**, 15–36.

Bourne H. L., Bishop J. K. B., Lam P. J. and Ohnemus D. C. (2018) Global spatial and temporal variation of Cd: P in euphotic zone particulates. *Global Biogeochem. Cycles* **32**, 1123–1142.

Boyle E. A. (1988) Cadmium: Chemical tracer of deepwater paleoceanography. *Paleoceanography* **3**, 471–489.

Boyle E. A., John S. G., Abouchami W., Adkins J. F., Echegoyen-Sanz Y., Ellwod M. E. and Zhao Y. (2012) GEOTRACES IC1 (BATS) contamination-prone trace element isotopes Cd, Fe, Pb, Zn, Cu and Mo intercalibration. *Limnol. Oceanogr. Methods* **10**, 653–665.

Boyle E. A., Sclater F. and Edmond J. M. (1976) On the marine geochemistry of cadmium. *Nature* **263**, 42–44.

Bruland K. W. (1980) Oceanographic distributions of cadmium, zinc, nickel, and copper in the North Pacific. *Earth Planet. Sci. Lett.* **47**, 176–198.

Bruland K. W. (1992) Complexation of cadmium by natural organic ligands in the central North Pacific. *Limnol. Oceanogr.* **37**, 1008–1017.

Bryan A. L., Dickson A. J., Dowdall F., Homoky W. B., Porcelli D. and Henderson G. M. (2021) Controls on the cadmium

isotope composition of modern marine sediments. *Earth Planet. Sci. Lett.* **565** 116946.
Canfield D., Stewart F. J., Thamdrup B., De Brabandere L., Dalsgaard T., DeLong E. F. and Ulloa O. (2010) A cryptic sulfur cycle in oxygen-minimum zone waters off the Chilean coast. *Science* **330**, 1375–1378.
Chen L., Little S. H., Kreissig K., Severmann S. and McManus J. (2021) Isotopically light Cd in sediments underlying oxygen deficient zones. *Front. Earth Sci.* **9** 623720.
Cloete R., Loock J. C., van Horsten N., Fietz S., Mtshali T. N., Planquette H. and Roychoudhury A. N. (2021) Winter biogeochemical cycling of dissolved and particulate cadmium in the Indian sector of the Southern Ocean (GEOTRACES GIpr07 transect). *Front. Mar. Sci.*.
Conway T. and John S. G. (2014) Quantification of dissolved iron sources to the North Atlantic Ocean. *Nature* **511**, 212–215.
Conway T. M. and John S. G. (2015a) Biogeochemical cycling of cadmium isotopes along a high-resolution section through the North Atlantic Ocean. *Geochim. Cosmochim. Acta* **148**, 269–283.
Conway T. M. and John S. G. (2015b) The cycling of iron, zinc and cadmium in the North East Pacific Ocean – Insights from stable isotopes. *Geochim. Cosmochim. Acta* **164**, 262–283.
Cullen J. T., Chase Z., Coale K. H., Fitzwater S. E. and Sherrell R. M. (2003) Effect of iron limitation on the cadmium to phosphorus ratio of natural phytoplankton assemblages from the Southern Ocean. *Limnol. Oceanogr.* **48**, 1079–1087.
Cutter G. A., Moffett J. W., Nielsdóttir M. C. and Sanial V. (2018) Multiple oxidation state trace elements in suboxic waters off Peru: in situ redox processes and advective/diffusive horizontal transport. *Mar. Chem.* **201**, 77–89.
de Baar H. J. W., Saager P. M., Nolting R. F. and van der Meer J. (1994) Cadmium versus phosphate in the world ocean. *Mar. Chem.* **46**, 261–281.
de Souza G. F., Reynolds B. C., Rickli J., Frank M., Saito M. A., Gerringa L. J. A. and Bourdon B. (2012) Southern Ocean control of silicon stable isotope distribution in the deep Atlantic Ocean. *Global Biogeochem. Cycles* **26**.
Debeljak P., Blain S., Bowie A., van der Merwe P., Bayer B. and Obernosterer I. (2021) Homeostatis drives intense microbial trace metal processing on marine particles. *Limnol. Oceanogr.* **66**, 3842–3855.
Dugdale R. C., Wischmeyer A. G., Wilkerson F. P., Barber R. T., Chai F., Jiang M. S. and Peng T. H. (2002) Meridional asymmetry of source nutrients to the equatorial Pacific upwelling ecosystem and its potential impact on ocean-atmosphere CO_2 flux; a data and modeling approach. *Deep Sea Res. Part II* **49**, 2513–2531.
Ellwood M. J. (2008) Wintertime trace metal (Zn, Cu, Ni, Cd, Pb and Co) and nutrient distributions in the Subantarctic Zone between 40–52°S; 155–160°E. *Mar. Chem.* **112**, 107–117.
Fiedler P. C. and Talley L. D. (2006) Hydrography of the eastern tropical Pacific: A review. *Prog. Oceanogr.* **69**, 143–180.
Finkel Z. V., Quigg A. S., Chiampi R. K., Schofield O. E. and Falkowski P. G. (2007) Phylogenetic diversity in cadmium : phosphorus ratio regulation by marine phytoplankton. *Limnol. Oceanogr.* **52**, 1131–1138.
Franz J., Krahmann G., Lavik G., Grasse P., Dittmar T. and Riebesell U. (2012) Dynamics and stoichiometry of nutrients and phytoplankton in waters influenced by the oxygen minimum zone in the eastern tropical Pacific. *Deep Sea Res. Part I* **62**, 20–31.
Frew R. D. (1995) Antarctic bottom water formation and the global cadmium to phosphorus relationship. *Geophys. Res. Lett.* **22**, 2349–2352.
Frew R. D. and Hunter K. A. (1992) Influence of Southern Ocean waters on the cadmium-phosphate properties of the global ocean. *Nature* **360**, 144–146.
Fripiat F., Martínez-García A., Marconi D., Fawcett S. E., Kopf S. H., Luu V. H. and Haug G. H. (2021) Nitrogen isotopic constraints on nutrient transport to the upper ocean. *Nat. Geosci.* **14**, 855–861.
George E., Stirling C. H., Gault-Ringold M., Ellwood M. J. and Middag R. (2019) Marine biogeochemical cycling of cadmium and cadmium isotopes in the extreme nutrient-depleted subtropical gyre of the South West Pacific Ocean. *Earth Planet. Sci. Lett.* **514**, 84–95.
Gruber N. and Sarmiento J. L. (1997) Global patterns of marine nitrogen fixation and denitrification. *Global Biogeochem. Cycles* **11**, 235–266.
Guinoiseau D., Galer S. J. G. and Abouchami W. (2018) Effect of cadmium sulphide precipitation on the partitioning of Cd isotopes: Implications for the oceanic Cd cycle. *Earth Planet. Sci. Lett.* **498**, 300–308.
Guinoiseau D., Galer S. J. G., Abouchami W., Frank M., Achterberg E. P. and Haug G. H. (2019) Importance of cadmium sulfides for biogeochemical cycling of Cd and its isotopes in oxygen deficient zones – a case study of the Angola Basin. *Global Biogeochem. Cycles* **33**.
Honjo S., Manganini S. J., Krishfield R. A. and Francois R. (2008) Particulate organic carbon fluxes to the ocean interior and factors controlling the biological pump: A synthesis of global sediment trap programs since 1983. *Prog. Oceanogr.* **76**, 217–285.
Ingall E. and Jahnke R. (1994) Evidence for enhanced phosphorus regeneration from marine sediments overlain by oxygen depleted waters. *Geochim. Cosmochim. Acta* **58**, 2571–2575.
Janssen D. J., Abouchami W., Galer S. J. G. and Cullen J. T. (2017) Fine-scale spatial and interannual cadmium isotope variability in the subarctic northeast Pacific. *Earth Planet. Sci. Lett.* **472**, 241–252.
Janssen D. J., Abouchami W., Galer S. J. G., Purdon K. B. and Cullen J. T. (2019) Particulate cadmium stable isotopes in the subarctic northeast Pacific reveal dynamic Cd cycling and a new isotopically light Cd sink. *Earth and Planetary Science Letters* **515**, 67–78.
Janssen D. J., Conway T. M., John S. G., Christian J. R., Kramer D. I., Pedersen T. F. and Cullen J. T. (2014) Undocumented water column sink for cadmium in open ocean oxygen-deficient zones. *Proc. Natl. Acad. Sci.* **111**, 6888–6893.
Janssen D. J., Sieber M., Ellwood M. J., Conway T. M., Barrett P. M., Chen X. and Jaccard S. L. (2020) Trace metal and nutrient dynamics across broad biogeochemical gradients in the Indian and Pacific sectors of the Southern Ocean. *Mar. Chem.* **221** 103773.
Jenkins W. J., Smethie, Jr, W. M., Boyle E. A. and Cutter G. A. (2015) Water mass analysis for the U.S. GEOTRACES (GA03) North Atlantic sections. *Deep Sea Res. Part II* **116**, 6–20.
John S. G., Helgoe J. and Townsend E. (2018) Biogeochemical cycling of Zn and Cd and their stable isotopes in the Eastern Tropical South Pacific. *Mar. Chem.* **201**, 256–262.
Johnson G. C. and McPhaden M. J. (1999) Interior pycnocline flow from the subtropical to the equatorial Pacific Ocean. *J. Phys. Oceanogr.* **29**, 3073–3089.
Johnson Z. I., Zinser E. R., Coe A., McNulty N. P., Woodward E. M. S. and Chisholm S. W. (2006) Niche partitioning among *Prochlorococcus* ecotypes along ocean-scale environmental gradients. *Science* **311**, 1737–1740.
Klar J. K., Schlosser C., Milton J. A., Woodward E. M. S., Lacan F., Parkinson I. J. and James R. H. (2018) Sources of dissolved iron to oxygen minimum zone waters on the Senegalese

continental margin in the tropical North Atlantic Ocean: insights from iron isotopes. *Geochim. Cosmochim. Acta* **236**, 60–78.

Lacan F., Francois R., Ji Y. and Sherrell R. M. (2006) Cadmium isotopic composition in the ocean. *Geochim. Cosmochim. Acta* **70**, 5104–5118.

Lane E. S., Semeniuk D. M., Strzepek R. F., Cullen J. T. and Maldonado M. T. (2009) Effects of iron limitation on intracellular cadmium of cultured phytoplankton: Implications for surface dissolved cadmium to phosphate ratios. *Mar. Chem.* **115**, 155–162.

Lane T. W. and Morel F. M. M. (2000) A biological function for cadmium in marine diatoms. *Proc. Natl. Acad. Sci.* **97**, 4627–4631.

Lee J.-M., Heller M. and Lam P. J. (2018) Size distribution of particulate trace elements in the US GEOTRACES Eastern Pacific Zonal Transect (GP16). *Mar. Chem.* **201**, 108–123.

Lee J. G. and Morel F. M. M. (1995) Replacement of zinc by cadmium in marine phytoplankton. *Mar. Ecol. Prog. Ser.* **127**, 305–309.

Lee J. G., Roberts S. B. and Morel F. M. M. (1995) Cadmium: a nutrient for the marine diatom *Thalassiosira weissflogii*. *Limnol. Oceanogr.* **40**, 1056–1063.

Letscher R. T. and Moore J. K. (2015) Preferential remineralization of dissolved organic phosphorus and non-Redfield DOM dynamics in the global ocean: Impacts on marine productivity, nitrogen fixation, and carbon export. *Global Biogeochem. Cycles* **29**, 325–340.

Little S. H., Vance D., Lyons T. W. and McManus J. F. (2015) Controls on trace metal authigenic enrichment in reducing sediments: insights from modern oxygen-deficient settings. *Am. J. Sci.* **315**, 77–119.

Marconi D., Weigand M. A., Rafter P. A., McIlvin M., Forbes M., Casciotti K. L. and Sigman D. M. (2015) Nitrate isotope distributions on the US GEOTRACES North Atlantic cross-basin section: signals of polar nitrate sources and low latitude nitrogen cycling. *Mar. Chem.* **177**, 143–156.

Martiny A. C., Pham C. T. A., Primeau F. W., Vrugt J. A., Moore J. K., Levin S. A. and Lomas M. W. (2013) Strong latitudinal patterns in the elemental ratios of marine plankton and organic matter. *Nat. Geosci.* **6**, 279–283.

McCartney M. S. (1982) The subtropical recirculation of Mode Waters. *J. Mar. Res.* **40**(Suppl.), 427–464.

Middag R., Séférian R., Conway T. M., John S. G., Bruland K. W. and de Baar H. J. W. (2015) Intercomparison of dissolved trace elements at the Bermuda Atlantic Time Series station. *Mar. Chem.* **177**, 476–489.

Middag R., van Heuven S. M. A. C., Bruland K. W. and de Baar H. J. W. (2018) The relationship between cadmium and phosphate in the Atlantic Ocean unravelled. *Earth Planet. Sci. Lett.* **492**, 79–88.

Moore C. M., Mills M. M., Arrigo K. R., Berman-Frank I., Bopp L., Boyd P. and Ulloa O. (2013) Processes and patterns of oceanic nutrient limitations. *Nat. Geosci.* **6**, 701–710.

Morel F. M. M. (2013) The oceanic cadmium cycle: biological mistake or utilization? *PNAS* **110**, E1877.

Morford J. L. and Emerson S. (1999) The geochemistry of redox sensitive trace metals in sediments. *Geochim. Cosmochim. Acta* **63**, 1735–1750.

Noffke A., Hensen C., Sommer S., Scholz F., Bohlen L., Mosch T. and Wallmann K. (2012) Benthic iron and phosphorus fluxes across the Peruvian oxygen minimum zone. *Limnol. Oceanogr.* **57**, 851–867.

Ohnemus D. C., Rauschenberg S., Cutter G. A., Fitzsimmons J. N., Sherrell R. M. and Twining B. S. (2017) Elevated trace metal content of prokaryotic communities associated with marine oxygen deficient zones. *Limnol. Oceanogr.* **62**, 3–25.

Ohnemus D. C., Torrie R. and Twining B. S. (2019) Exposing the distributions and elemental associations of scavenged particulate phases in the ocean using basin-scale multi-element data sets. *Global Biogeochem. Cycles* **33**, 725–748.

Peters B., Lam P. J. and Casciotti K. L. (2018) Nitrogen and oxygen isotope measurements of nitrate along the US GEOTRACES Eastern Pacific Zonal Transect (GP16) yield insights into nitrate supply, remineralization, and water mass transport. *Mar. Chem.* **201**, 137–150.

Plass A., Schlosser C., Sommer S., Dale A. W., Achterberg E. A. and Scholz F. (2020) The control of hydrogen sulfide on benthic iron and cadmium fluxes in the oxygen minimum zone off Peru. *Biogeosciences* **17**, 3685–3704.

Plass A., Dale A. W. and Scholz F. (2021) Sedimentary cycling and benthic fluxes of manganese, cobalt, nickel, copper, zinc and cadmium in the Peruvian oxygen minimum zone. *Marine Chemistry* **233** 103982.

Price N. M. and Morel F. M. M. (1990) Cadmium and cobalt substitution for zinc in a marine diatom. *Nature* **344**, 658–660.

Quay P., Cullen J. D., Landing W. M. and Morton P. (2015) Processes controlling the distributions of Cd and PO4 in the ocean. *Global Biogeochem. Cycles* **29**, 830–841.

Quay P. and Wu J. (2015) Impact of end-member mixing on depth distributions of $\delta^{13}C$, cadmium and nutrients in the N. Atlantic Ocean. *Deep Sea Res. Part II* **116**, 107–116.

Raven M. R., Keil R. G. and Webb S. M. (2021) Microbial sulfate reduction and organic sulfur formation in sinking marine particles. *Science* **371**, 178–181.

Redfield A. C. (1934) *On the proportions of organic derivatives in sea water and their relation to the composition of plankton*. James Johnstone Memorial Volume, Liverpool, pp. 176–192.

Reid J. L. (1997) On the total geostrophic circulation of the Pacific Ocean: flow patterns, tracers, and transports. *Prog. Oceanogr.* **39**, 263–352.

Rijkenberg, M.J.A. (2011) Cruise Report JC057 on RRS James Cook: GEOTRACES West Atlantic Leg 3. GEOTRACES / Royal NIOZ, p. 92.

Ripperger S., Rehkämper M., Porcelli D. and Halliday A. N. (2007) Cadmium isotope fractionation in seawater – A signature of biological activity. *Earth Planet. Sci. Lett.* **261**, 670–684.

Roshan S. and DeVries T. (2021) Global contrasts between oceanic cycling of cadmium and phosphate. *Global Biogeochem. Cycles* **35**, e2021GB006952.

Roshan S. and Wu J. (2015) Cadmium regeneration within the North Atlantic. *Global Biogeochem. Cycles* **29**, 2082–2094.

Roshan S., Wu J. and DeVries T. (2017) Controls on the cadmium-phosphate relationship in the tropical South Pacific. *Global Biogeochem. Cycles* **31**, 1516–1527.

Ruppert K. M., Kline R. J. and Rahman M. S. (2019) Past, present, and future perspectives of environmental DNA (eDNA) metabarcoding: A systematic review in methods, monitoring, and applications of global eDNA. *Global Ecol. Conserv.* **17** e00547.

Saager P. M. and de Baar H. J. W. (1993) Limitations to the quantitative application of Cd as a paleoceanographic tracer, based on results of a multi-box model (MENU) and statistical considerations. *Global Planet. Change* **8**, 69–92.

Saito M. A., Sigman D. M. and Morel F. M. M. (2003) The bioinorganic chemistry of the ancient ocean: the co-evolution of cyanobacterial metal requirements and biogeochemical cycles at the Archean-Proterozoic boundary. *Inorg. Chim. Acta* **356**, 308–318.

Sarmiento J. L., Gruber N., Brzezinski M. A. and Dunne J. P. (2004) High-latitude controls of thermocline nutrients and low latitude biological productivity. *Nature* **427**, 56–60.

Sarmiento J. L., Simeon J., Gnanadesikan A., Gruber N., Key R. M. and Schlitzer R. (2007) Deep ocean biogeochemistry of silicic acid and nitrate. *Global Biogeochem. Cycles* **21**.

Schlitzer, R. (2019) Ocean Data View, https://odv.awi.de, 5 ed.

Schlitzer R., Anderson R. F., Dodas E. M., Lohan M., Geibert W., Tagliabue A. and Zurbrick C. (2018) The GEOTRACES Intermediate Data Product 2017. *Chem. Geol.* **493**, 210–223.

Schmittner A., Gruber N., Mix A. C., Key R., Tagliabue A. and Westberry T. K. (2013) Biology and air-sea gas exchange controls on the distribution of carbon isotope ratios $\delta^{13}C$) in the ocean. *Biogeosciences* **10**, 5793–5816.

Schott, F., McCreary, J.P. and Johnson, G.C. (2004) Shallow overturning circulations of the tropical-subtropical oceans, in: Wang, C., Xie, S.P., Carton, J.A. (Eds.), *Earth's Climate: The Ocean-Atmosphere Interaction*, pp. 261-304.

Schroller-Lomnitz U., Hensen C., Dale A. W., Scholz F., Clemens D., Sommer S. and Wallmann K. (2019) Dissolved benthic phosphate, iron and carbon fluxes in the Mauritanian upwelling system and implications for ongoing deoxygenation. *Deep Sea Res. Part I* **143**, 70–84.

Schunck H., Lavik G., Desai D. K., Grosskopf T., Kalvelage T., Löscher C. R. and LaRoche J. (2013) Giant hydrogen sulfide plume in the oxygen minimum zone off Peru supports chemolithoautotrophy. *PLoS ONE* **8** e68661.

Sherrell R. M. (1989) *The Trace Metal Geochemistry of Suspended Oceanic Particulate Matter*. MIT/WHOI, Ph.D. thesis.

Sieber M., Conway T. M., de Souza G. F., Hassler C. S., Ellwood M. and Vance D. (2019a) High-resolution Cd isotope systematics in multiple zones of the Southern Ocean from the Antarctic Circumnavigation Expedition. *Earth Planet. Sci. Lett.* **527** 115799.

Sieber M., Conway T. M., de Souza G. F., Obata H., Takano S., Sohrin Y. and Vance D. (2019b) Physical and biogeochemical controls on the distribution of dissolved cadmium and its isotopes in the Southwest Pacific Ocean. *Chem. Geol.* **511**, 494–509.

Sipler R. E. and Bronk D. A. (2015) Dynamics of Dissolved Organic Nitrogen. In *Biogeochemistry of Marine Dissolved Organic Matter* (eds. D. A. Hansell and C. A. Carlson). Academic Press, Burlington, pp. 127–232.

Sunda W. G. and Huntsman S. A. (1998) Control of Cd concentrations in a coastal diatom by interactions among free ionic Cd, Zn and Mn in seawater. *Environ. Sci. Technol.* **32**, 2961–2968.

Sunda W. G. and Huntsman S. A. (2000) Effect of Zn, Mn, and Fe on Cd accumulation in phytoplankton: Implications for oceanic Cd cycling. *Limnol. Oceanogr.* **45**, 1501–1516.

Tiano L., Garcia-Robledo E., Dalsgaard T., Devol A. H., Ward B. B., Ulloa O. and Peter Revsbech N. (2014) Oxygen distribution and aerobic respiration in the north and south eastern tropical Pacific oxygen minimum zones. *Deep Sea Res. Part I* **94**, 173–183.

Tsuchiya M. and Talley L. (1996) Water-property distributions along an eastern Pacific hydrographic section at 135W. *J. Mar. Res.* **54**, 541–564.

Twining B. S. and Baines S. B. (2013) The trace metal composition of marine phytoplankton. *Ann. Rev. Mar. Sci.* **5**, 191–215.

Twining, B.S., Rauschenberg, S., Morton, P.L. and Vogt, S. (2015) Metal contents of phytoplankton and labile particulate material in the North Atlantic Ocean. *Progress in Oceanography* **137, Part A**, 261-283.

Ulloa O., Canfield D. E., DeLong E. F., Letelier R. M. and Stewart F. J. (2012) Microbial oceanography of anoxic oxygen minimum zones. *Proc. Natl. Acad. Sci.* **109**, 15996–16003.

Vance D., Little S. H., de Souza G. F., Khatiwala S., Lohan M. C. and Middag R. (2017) Silicon and zinc biogeochemical cycles coupled through the Southern Ocean. *Nat. Geosci.* **10**, 202–206.

Vu H. T. D. and Sohrin Y. (2013) Diverse stoichiometry of dissolved trace metals in the Indian Ocean. *Sci. Rep.* **3**.

Waeles M., Maguer J.-F., Baurand F. and Riso R. D. (2013) Off Congo waters (Angola Basin, Atlantic Ocean): A hot spot for cadmium-phosphate fractionation. *Limnol. Oceanogr.* **58**, 1481–1490.

Waeles M., Planquette H., Afandi I., Delebecque N., Bouthir F., Donval A. and de Morais L. T. (2016) Cadmium in the waters off South Morocco: nature of particles hosting Cd and insights into the mechanisms fractionating Cd from phosphate. *Journal of Geophysical Research –. Oceans* **121**, 3106–3120.

Wang W.-L., Moore J. K., Martiny A. C. and Primeau F. (2019) Convergent estimates of marine nitrogen fixation. *Nature* **566**, 205–211.

Weber T. S. and Deutsch C. (2010) Ocean nutrient ratios governed by plankton biogeography. *Nature* **467**, 550–554.

Wu J. and Roshan S. (2015) Cadmium in the North Atlantic: Implication for global cadmium–phosphorus relationship. *Deep Sea Res. Part II* **116**, 226–239.

Xie R. C., Galer S. J. G., Abouchami W. and Frank M. (2019a) Limited impact of eolian and riverine sources on the biogeochemical cycling of Cd in the tropical Atlantic. *Chem. Geol.* **511**, 371–379.

Xie R. C., Galer S. J. G., Abouchami W., Rijkenberg M. J. A., de Baar H. J. W., De Jong J. and Andreae M. O. (2017) Non-Rayleigh control of upper-ocean Cd isotope fractionation in the western South Atlantic. *Earth Planet. Sci. Lett.* **471**, 94–103.

Xie R. C., Galer S. J. G., Abouchami W., Rijkenberg M. J. A., De Jong J., de Baar H. J. W. and Andreae M. O. (2015) The cadmium–phosphate relationship in the western South Atlantic — The importance of mode and intermediate waters on the global systematics. *Mar. Chem.* **177**, 110–123.

Xie R. C., Rehkämper M., Grasse P., van de Flierdt T., Frank M. and Xue Z. (2019b) Isotopic evidence for complex biogeochemical cycling of Cd in the eastern tropical South Pacific. *Earth Planet. Sci. Lett.* **512**, 134–146.

Xu Y., Tang D., Shaked Y. and Morel F. M. M. (2007) Zinc, cadmium, and cobalt interreplacement and relative use efficiencies in the coccolithophore Emiliania huxleyi. *Limnol. Oceanogr.* **52**, 2294–2305.

Xue Z., Rehkämper M., Horner T. J., Abouchami W., Middag R., van de Flierdt T. and de Baar H. J. W. (2013) Cadmium isotope variations in the Southern Ocean. *Earth Planet. Sci. Lett.* **382**, 161–172.

Yang S.-C., Zhang J., Sohrin Y. and Ho T.-Y. (2018) Cadmium cycling in the water column of the Kuroshio-Oyashio Extension region: Insights from dissolved and particulate isotopic composition. *Geochim. Cosmochim. Acta* **233**, 66–80.

Associate editor: Claudine Stirling